New Non-invasive Methods for Quantification of Regional and Global Myocardial Function in the Normal and Ischemic Left Ventricle

Thomas M. Helle-Valle, MD

Institute for Surgical Research and Department of Cardiology
Oslo University Hospital, Rikshospitalet and
Faculty of Medicine, University of Oslo
Oslo, Norway

2013

© Thomas M. Helle-Valle, 2013

Series of dissertations submitted to the
Faculty of Medicine, University of Oslo
No. 1559

ISBN 978-82-8264-502-7

All rights reserved. No part of this publication may be
reproduced or transmitted, in any form or by any means, without permission.

Cover: Inger Sandved Anfinsen.
Printed in Norway: AIT Oslo AS.

Produced in co-operation with Akademika publishing.
The thesis is produced by Akademika publishing merely in connection with the thesis defence. Kindly direct all inquiries regarding the thesis to the copyright holder or the unit which grants the doctorate.

Contents

Acknowledgements

The present thesis is based on studies carried out at the Department of Cardiology and at the Institute for Surgical Research, Oslo University Hospital, Rikshospitalet, during the years 2004 – 2007, and at Johns Hopkins University Hospital, Baltimore, USA, during the years 2007-2008.

The work was supported by the Norwegian Council of Cardiovascular Diseases from 2003 - 2006 and by the Department of Cardiology, Rikshospitalet, from 2006 - 2007. In addition, without the financial support from Medinnova AS, Unger-Vetlesen Foundation, Gidske og Peter Jacob Sørensens Foundation, Alf og Aagot Helgesens Foundation, Dr Alexander Malthes Foundation, Caroline Musæus Aarsvolds Foundation and from the Norwegian Society of Cardiology, an immensely informative and inspiring year as a research fellow at Johns Hopkins University Hospital would not have been possible.

The success of scientific research depends on the teamwork of individuals with complementary skills. The present thesis is the result of such teamwork. First of all, I have been extremely privileged to have had Professor Otto A. Smiseth as my formal supervisor since 2006. Otto is one of the world's foremost authorities on cardiovascular mechanics and his academic achievements are recognized worldwide. To work with Otto has been immensely inspiring and without his vast knowledge, bright ideas, enthusiasm, support and patience, my scientific achievements would simply not have been possible. Despite Otto's busy schedule, he has always been available for encouraging discussions, even if that sometimes meant short meetings during coffee breaks at conferences, in hotel lobbies, at airports, or while walking with him to his next meeting. Nevertheless, because of Otto's ability to focus and to extract the scientific essence of our data, even short meetings were highly productive. I also wish to thank Otto for giving me the opportunity to spend an unforgettable and highly informative year as a research fellow at Johns Hopkins University Hospital.

Professor Thor Edvardsen became my co-supervisor in 2006. His knowledge within the field of cardiac imaging, his experience in experimental and clinical research and his ability to overcome the practical difficulties frequently met while carrying out various research projects, were absolutely essential to my research. Despite his busy schedule, his open door policy frequently initiated spontaneous and

highly fruitful discussions – sometimes even on non-scientific topics. I also wish to thank Thor for his generosity and friendship.

I was fortunate to have Professor Halfdan Ihlen as my formally supervisor until his retirement in 2006. Halfdan has a unique position in Norwegian cardiology and have played a central role in the development of various echocardiographic techniques. His experience with both clinical work and research, his personal qualities, his enthusiasm for our scientific work, his encouragements during adversities and his focus on the balance between independent and cooperative work, made him to an outstanding mentor.

The experimental research performed at Institute for Surgical Research was complex and time consuming and required 100% teamwork. Without the genuine knowledge, support and advices of my colleagues and friends Anders Opdahl, Espen Remme, Trond Vartdal, Erik Lyseggen, Eirik Pettersen and Helge Skulstad, the experimental part of my research would not have been possible. The development and use of complex mathematical models and algorithms were a central part of my research. Thanks to engineers Espen Remme, Jonas Crosby and Stein-Inge Rabben these issues were elegantly solved. I also wish to thank Drs Ketil Lunde, Ola Gjesdal, Einar Hopp and Hans-Jørgen Smith for important and generous contributions. I am also indebted to Dr Brage H Amundsen and Professor Hans Torp from Department of Circulation and Medical Imaging, NTNU, for their important contributions to Paper 1 in the present thesis. Thanks to the statistician Are Hugo Pripp for helping me with the linear mixed-model statistical method in Paper 2.

I feel much honored to have had the opportunity to be a part of Professor João A. C. Lima's research team at Johns Hopkins University Hospital in Baltimore. João is heading one of the world's leading centers when it comes to cardiac imaging and the use of MRI and CT. His personal qualities are unique and the invaluable experiences I gained as a research fellow are too many to be listed. Due to João's support, enthusiasm, humor and friendship, I am looking forward to continuing our ongoing scientific collaboration. I would also like to express my deepest gratitude to my great colleagues and friends at Johns Hopkins University Hospital, Drs Veronica Fernandes, Boas D. Rosen, Wen-Chung Yu, Ilan Gottlieb, Andrea Vavere and engineer Elzbieta Chamera. Their enthusiasm, support and cooperation were essential for the development of the new multimodality tissue tracking method and the

subsequent publication (Paper 3 in my Thesis). A special thanks to Kathleen Lensch for solving any problem at any time.

Thanks to Professor Ansgard Aasen for office facilities and for providing a stimulating environment at the Institute for Surgical Research; to Vivi Bull Stubberud for keeping the operation room in order; to Roger Ødegård and Eldrid Winther-Larssen for technical assistance; and to Dr Svend Aakhus, Pia Bryde, Johanna Andreassen and Richard Massey at the Echo-lab for, among other tasks, helping me improving my echocardiographic imaging skills.

Finally, I wish to thank my loving and inspiring parents, who passed away too early, but who still live inside of me; my family and friends for vitalizing my life; and my parents-in-law for their generosity and support whenever needed. Last, but not least, my deepest gratitude goes to my wife Anita and to our daughters Sara and Maja for reminding me every day that there is more to the heart than strain, torsion and twist - I love you!

List of papers

I. Helle-Valle T, Crosby J, Edvardsen T, Lyseggen E, Amundsen BH, Smith HJ, Rosen BD, Lima JA, Torp H, Ihlen H, Smiseth OA. New Noninvasive Method for Assessment of Left Ventricular Rotation: Speckle Tracking Echocardiography. Circulation. 2005; 112; 3149-3156.

II. Helle-Valle T, Remme EW, Lyseggen E, Pettersen E, Vartdal T, Opdahl A, Smith HJ, Osman N, Ihlen H, Edvardsen T, Smiseth OA. Clinical Assessment of Left Ventricular Rotation and Strain – A Novel Approach for Quantification of Function in Infarcted Myocardium and its Border Zones. Am J Physiol Heart Circ Physiol. 2009 Jul;297(1):H257-67

III. Helle-Valle T; Yu WC; Fernandes VRF; Rosen BD; Lima JAC. Usefulness of Radial Strain Mapping by Multidetector Computer Tomography (MDCT) to Quantify Regional Myocardial Function in Patients with Healed Myocardial Infarction. Am J Cardiol. 2010 Aug 15;106(4):483-91.

Selected Abbreviations

2-D = two-dimensional

CVD = cardiovascular disease

ECG = electrocardiogram

ED = end-diastole

ES = end-systole

ICD = implantable cardioverter-defibrillator

dP/dt = time derivative of left ventricular pressure

LAD = left anterior descending coronary artery

LE MRI = late enhancement magnetic resonance imaging

LV = left ventricle/left ventricular

LVP = left ventricular pressure

MDCT = multidetector computer tomography

MRI = magnetic resonance imaging

MTT = multimodality tissue tracking

RCA = right coronary artery

ROI = region of interest

STE = speckle tracking echocardiography

Introduction

Left ventricular (LV) dysfunction is a progressive and malignant condition and among the leading causes of morbidity and mortality worldwide. Optimal handling strategies for patients with suspected or established LV dysfunction depend on the ability to determine its mechanism and extent and non-invasive methods for assessment of LV function are therefore pivotal. However, normal LV function is a highly complex sequence of multiple interrelated events involving factors such as active and passive myocardial tissue properties, coordinated electro-mechanical coupling, loading conditions, geometry and LV fiber orientation. Because cardiovascular diseases, such as coronary artery disease, arrhythmias, hypertension, diabetes, valvular disease, myocarditis, congenital heart disease and cardiomyopathies may affect LV function through different mechanisms, an unambiguous definition of LV dysfunction is difficult. Consequently, non-invasive modalities that allow accurate and reproducible quantification of markers reflecting different aspects of LV mechanics and function are needed.[1-4] *The aim of the present Thesis is to introduce new non-invasive quantitative methods for assessment of regional and global LV function and to use these methods to study LV mechanics in the setting of myocardial ischemia, the most common cause of LV dysfunction.*

Normal LV deformation

At the macroscopic level, normal LV systolic function is the result of LV deformation caused by synchronous contraction of myocardial fibers of different orientations (Figure 1).

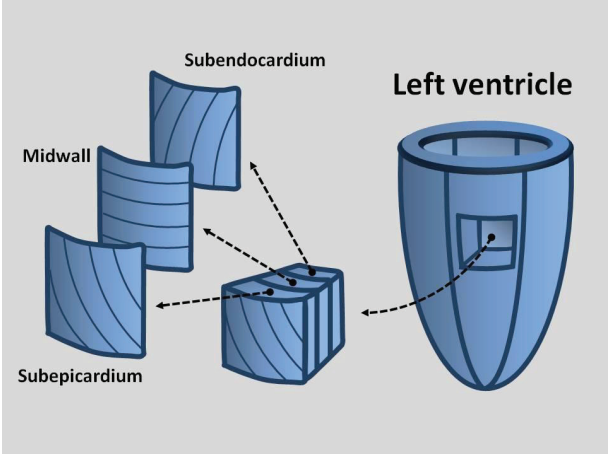

Figure 1. *LV myocardial fiber orientation changes gradually from a left-handed helix in the subepicardium to a right-handed helix in the subendocardium. In the midwall, myocardial fibers are essentially circumferentially oriented*

By convention, myocardial deformation is expressed along 3 perpendicular LV axes; longitudinal, circumferential and radial (Figure 2, left panel).[5] During systole, the longitudinal component of LV fiber shortening causes the LV base to descend towards the apex, while the circumferential component causes reduction of LV short-axis diameter, both mechanisms contributing to systolic wall thickening and, consequently, a reduction in LV cavity volume. In addition, due to contraction of obliquely oriented fibers, there is a torsional deformation of the LV about its long-axis.

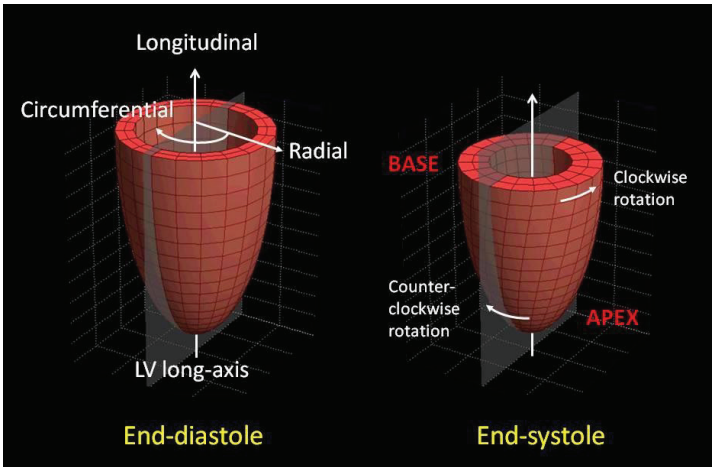

Figure 2. *Schematic illustration of the three LV deformation axes (left panel) and of LV torsional deformation, including clockwise rotation of the base, when viewed from the apex, and counter-clockwise rotation of the apex (right panel).*

In the subepicardium the oblique fibers course towards the base in a counter-clockwise spiral (viewed from the apex), and in the subendocardium they form an oppositely directed spiral. Because of larger radii and mass the subepicardial fibers dominate and account for the normal LV apex-to-base rotation gradient (torsion), including counter-clockwise rotation of the LV apex and clockwise rotation of the base (Figure 2, right panel).

Current methods for assessment of LV function

LV deformation is the sum of regional myocardial contractions. Because certain cardiac diseases, such as ischemic heart disease, are regional by nature, and regional dysfunction not necessarily reduces global function due to compensatory mechanisms, markers of both global and regional LV function are needed. Given the complexity of LV systolic deformation, simplified markers of LV function have been used. Current markers utilize the reduction in cavity volume caused by inward motion of the endocardium during LV systolic ejection. Calculation of LV volumes and ejection fraction (EF), the percentage of cavity volume ejected during systole, and visual

evaluation of LV regional wall motion (wall motion score index) and thickening are therefore the most widely used markers of global and regional LV function. These markers can be measured non-invasively from cine loops obtained by transthoracic echocardiography, magnetic resonance imaging (MRI) or multidetector computed tomography (MDCT). The most widely used modality is echocardiography, which is a bedside technique that is highly available, portable, safe and inexpensive and allows for real-time visualization of cardiac morphology, hemodynamics and motion.

In patients with poor acoustic window, MRI and MDCT are alternatives to echocardiography for assessment of LV volumes and wall motion. Cardiac MRI has been considered the clinical "gold standard" but is a complex, expensive and time consuming modality of limited availability that cannot be performed in patients with implanted pacemakers or defibrillators. MDCT has recently emerged as a promising noninvasive clinical tool for assessment of cardiac morphology, coronary anatomy and myocardial perfusion, viability and scarring.[6, 7] Retrospective ECG-gated MDCT allows for image reconstruction in any phase of the cardiac cycle and, thus, for construction of cine loops. Recent studies have demonstrated that LV volumes, wall motion and wall thickening can be assessed accurately when compared to measures by MRI, echocardiography and SPECT.[8, 9] MDCT has the advantage of being fast, relatively inexpensive and providing images of high spatial resolution. Although radiation is an important limitation, the introduction of new generations multidetector and dual source MDCT scanners have dramatically reduced this problem.[10]

Echocardiographic assessment of LV volumes, EF, wall motion and thickening has proven to be clinically useful in most cardiac diseases. The method, however, has important limitations by being subjective, highly observer and image quality dependent, insensitive to subtle changes in myocardial function and predominantly reflecting the radial component of myocardial deformation.[11-14] Due to the progressive nature of LV dysfunction and the potential benefit of early detection, quantitative markers of subtle, subclinical myocardial dysfunction are needed. Studies have shown that changes in the normal temporal pattern of the LV deformation sequence, particularly in the setting of myocardial ischemia or dyssynchrony, precedes changes in the amplitude of wall motion and wall thickening.[15-17] Consequently, there is a need for additional methods for non-invasive quantification of the magnitude and timing of regional and global myocardial deformation.

Measures of LV deformation

Strain is a measure of deformation introduced to describe LV wall stiffness in terms of myocardial deformation following application of stress.[18] In general terms, strain represents the fractional or percentage change in dimension and is defined as tissue elongation relative to length, usually end-diastolic (Langrangian strain; Figure 3) or instantaneous length (Eulerian strain). Positive strain refers to elongation and negative strain to shortening. Strain is a vector that can be measured along any given axis. Because LV systolic deformation involves longitudinal and circumferential shortening and radial thickening, quantification of myocardial strain along these axes represent a measure of contractile function.

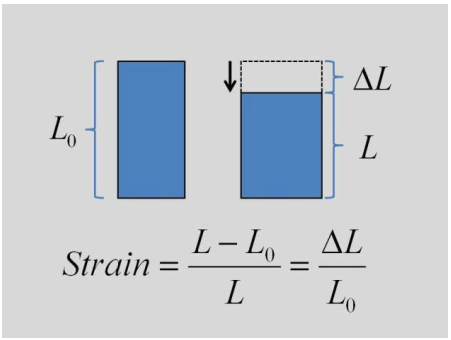

Figure 3. *Strain is a measure of how much an object has been deformed, and several formulas can be used to calculate different types of strain. In cardiac mechanics we use the simple approach and calculate strain as percent or fractional change in dimension. In the formula L is the current length and L_0 is the original length.*

Strain can be measured by sonomicrometry[19] and MRI-tagging[20] and important insights into LV myocardial deformation under various pathophysiological settings have been provided by these methods. However, due to methodological limitations they are only used for research purposes. Strain by tissue-Doppler echocardiography was introduced a decade ago by Urheim et al,[21] but the method has not reached widespread clinical use due to high intra- and interobserver variability and to measurements restricted to ultrasound beam direction.

Another aspect of LV function is the torsional deformation caused by the base-to-apex rotation gradient. Unfortunately, the terms used to describe the circumferential-longitudinal shear deformation of the LV have been confusing and *rotation*, *twist* and *torsion* are often used interchangeably.[22] However, LV *rotation* refers to the angle between radial lines connecting specific points in the myocardial wall of a specific short-axis plane to the centre of the same short-axis plane at end-diastole and at any other time point throughout the cardiac cycle (Figure 4). Because LV torsional deformation reflects circumferential-longitudinal shear, the distance between two short-axis planes is relevant. *Twist* refers to the difference in rotation between two short-axis planes at isochronal time points without taking into account the distance between the

two planes, while *torsion* refers to the rotational difference between two short-axis planes (twist) when normalized to the instantaneous distance between the two planes. Because the dynamic distance between apical and basal short-axis planes is difficult to assess by 2-dimensional echocardiography, the terms torsion and twist are frequently used synonymously. *For simplicity, in the present Thesis, LV rotation is used as a common term for LV rotation, twist and torsion unless stated otherwise.*

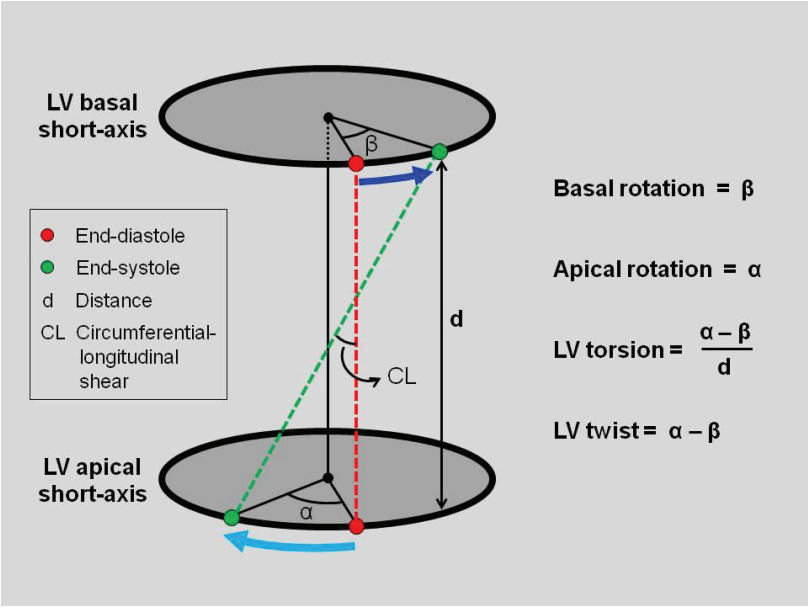

Figure 4. *Cylindrical LV model illustrating direction and magnitude of basal (dark blue arrow) and apical (light blue arrow) rotation. Because the dynamic distance between apical and basal short-axis planes is difficult to measure by 2-dimensional echocardiography, in Paper 1, LV torsion was calculated simply as the rotational difference between apical and basal rotation (i.e. twist).*

The magnitude and characteristics of LV rotation have been described in different clinical and experimental studies using MRI- tagging and other complex methodologies.[23-29] It is well established that LV rotation is sensitive to changes in both regional and global LV function,[25, 30-41] and an important marker with respect to LV ejection and filling.[30, 42-45] Although LV rotation reflects a fundamental property of normal LV function and has been proposed as a useful clinical marker of impaired LV function,[39, 46-51] LV rotation has not been incorporated into the clinical assessment of LV function due to methodological limitations.

Assessment of LV deformation

At the initiation of the present studies, speckle tracking echocardiography (STE) had recently been introduced as a promising angle-independent method for automated tracking of natural acoustic markers (speckles) visualized by conventional gray-scale imaging.[52, 53] Because speckles represent myocardial "finger prints" and can be tracked in any direction throughout the cardiac cycle (Figure 5), myocardial motion and deformation can be measured by STE in the circumferential and radial direction from LV short axis recordings, and in the longitudinal and transversal direction from LV long axis recordings. Consequently, the introduction of STE as a non-invasive method to quantify LV motion and deformation represented an important breakthrough which allowed for LV strain and rotation to be brought into the clinical arena.

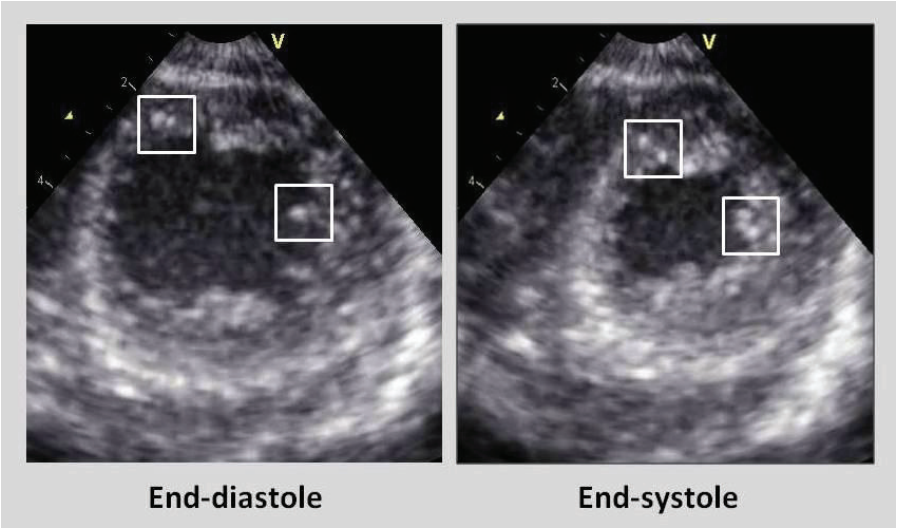

Figure 5. *End-diastolic and end-systolic apical short-axis echocardiographic images from an animal experiment. Stable speckle patterns or "finger prints" suitable for automated tracking are indicated (white squares) at end-diastole (left panel) and end-systole (right panel).*

Recently, Ogawa et al[54] introduced another echocardiographic speckle tracking algorithms based on automated tracking of "on-screen" pixel patterns. Because the algorithm uses cine loops stored in the AVI format, it does not discriminate between different imaging modalities and, thus, represented a promising multimodality technique for automated tracking of myocardial motion and deformation.

Assessment of LV function during Myocardial Infarction

Myocardial ischemia caused by coronary artery stenosis or occlusion is the most common cause of LV dysfunction and involves a wide spectrum of pathophysiological conditions, ranging from acute ischemia to chronic infarction. Detection and quantification of myocardial ischemia provides important diagnostic, therapeutic and prognostic information in both the acute and chronic phases, even when the initial event was not recognized.[55] Detection of reversibly injured myocardium in the setting of acute (stunning) or chronic (hibernation) ischemia and assessment of total infarct size and transmurality are important in order to determine potential benefit from revascularization,[56-58] and for prediction of long-term improvement in contractile function.[59, 60] Recent studies have also emphasized the prognostic importance of quantifying the infarct border zone (peri-infarct zone) in addition to infarct core, as the former is a substrate for malignant ventricular arrhythmias and its extent an independent marker of sudden death.[61]

Late-enhanced contrast MRI is the reference method for accurate visualization and quantification of myocardial scarring,[62] but clinical use is limited by restricted availability. An indirect way of measuring infarct extent is to study its effects on myocardial deformation. Changes in myocardial contraction patterns caused by ischemia were first elegantly demonstrated by Tennant and Wiggers in 1935.[63] Impaired systolic contraction patterns are observed within seconds of acute ischemia and characteristic changes in the magnitude and timing of myocardial deformation occur as myocardial infarction evolves as a wavefront of necrosis extending from the subendocardium to the subepicardium within hours.[64, 65] In patients with suspected or established ischemic heart disease, non-invasive assessment of LV regional and global deformation has proven to be relevant with respect to diagnosis, treatment selection and prognosis, as mortality increases exponentially with decreasing LVEF and linearly with increasing wall motion abnormality.[66] However, the sensitivity and specificity of determining ischemia visually by conventional echocardiography are moderate and show substantial variability in evaluating the extent and severity of regional dysfunction.[67, 68] Because of loading conditions and remodeling, low LVEF does not necessarily reflect the extent of reduced contractile function due to compensatory regional hyperkinesis or mitral regurgitation.[14] Similarly, regional wall motion might be misleading owing to viable but dysfunctional myocardium.

Furthermore, because myocardial infarcts demonstrate a highly irregular morphology and abrupt changes in infarct transmurality are commonly present,[69, 70] methods that allow accurate mapping of total infarct size and distribution from function analysis are needed.

Summary

Optimal handling strategies for patients with suspected or established cardiac disease require non-invasive methods for assessment of the extent and mechanism of LV dysfunction. Although current volumetric and wall motion indices by echocardiography, cardiac MRI or MDCT are useful, additional quantitative and sensitive methods for assessment of myocardial mechanics are needed. Functional analysis is of particular importance in the setting of myocardial ischemia, the most common cause of LV dysfunction. In the present Thesis we introduce and validate LV rotation and strain by STE, and radial strain mapping by multimodality tissue tracking MDCT, as new non-invasive methods for quantitative assessment of the magnitude and timing of regional and global LV deformation. By detailed analysis of regional strain and rotation in the infarcted LV, we demonstrate how ischemic and non-ischemic myocardium affects regional and global deformation indices and how these novel methods can be applied in a clinical setting.

Aims of the Thesis

General aims

To introduce new non-invasive methods for quantitative assessment of regional and global LV function, and to study myocardial function in the infarcted LV

Specific aims

- To introduce and validate speckle tracking echocardiography (STE) as a noninvasive method for assessment of LV rotation and torsion (Paper I)

- To determine how LV rotation and circumferential strain by STE can be used in combination to assess myocardial function in the infarcted LV (Paper II)

- To introduce and validate radial strain mapping by multimodality tissue tracking multidetector computer tomography (MDCT) as a new noninvasive method for quantification of myocardial function (Paper III)

- To investigate whether radial strain mapping by MDCT can be used to assess myocardial infarct distribution in patients with healed myocardial infarction (Paper III)

Material

Experimental Study

Paper I

Thirteen mongrel dogs of either sex were studied. Baseline data were obtained from all animals, whereas dobutamine intervention was not performed in the first 4 experiments. In 5 dogs, recordings during ischemia could not be obtained due to sustained ventricular fibrillation shortly after LAD occlusion. To explore the importance of an intact pericardium for LV rotation, short-axis recordings by STE were performed immediately before and after pericardiotomy in 6 dogs. The study was approved by the National Animal Experimentation Board and the animals were supplied by the Center for Comparative Medicine, Oslo University Hospital, Rikshospitalet.

Clinical Studies

Paper I

The study population consisted of 29 healthy volunteers (14 women; 33±6 years). The study protocol was approved by the National Committee for Medical Research Ethics of Norway and all participants gave written, informed consent.

Paper II

The study population consisted of 15 healthy volunteers (7 women; 34±7 years) and 23 patients selected from a database at OUS, Rikshospitalet, consisting of patients reexamined ~6 months after percutaneous coronary intervention (PCI) due to first time acute ST-elevation myocardial infarction. All patients with single coronary artery disease and echocardiographic short-axis recordings of the LV apex obtained from the apical window were included. According to angiographic findings, 18 patients had left descending coronary artery occlusion, 3 had circumflex coronary artery occlusion, and 2 had right coronary artery occlusion. All study subjects had given written, informed consent, and the protocol was approved by the Regional Ethics Committee.

Paper III

Available multidetector computer tomography (MDCT) data from patients with ischemic heart disease (n=20; 7 women; 56±11 years) who participated in a previously performed study at Johns Hopkins University Hospital, Baltimore, involving subjects with ischemic or idiopathic LV dysfunction were selected. These patients were referred for implantable cardioverter-defibrillator (ICD) placement and scheduled to undergo magnetic resonance (MR) imaging and MDCT imaging as part of a prospective study relating image patterns to ICD firings. All subjects had given written, informed consent and the study protocol was approved by the Johns Hopkins institutional review committee.

Methods

Experimental Study

Animal Model

The animal model used in Paper I is a well established model for integrated studies of cardiac mechanics and hemodynamics.[71-73] The reasons for using dogs, is their tolerance to extensive instrumentation, the appropriate size of the heart and the anatomical and functional resemblance to the human heart. The dogs were anesthetized, artificially ventilated and cannulated. After a median sternotomy, the pericardium was split and the edges of the pericardial incision were loosely resutured after instrumentation. Inflatable vascular occluders were placed around the proximal third of the LAD. Invasive pressure data were digitized at 200Hz. Recordings were obtained with the dogs in a supine position and with the ventilator turned off. At the end of the experiment, the animal was euthanized with an intracardiac injection of pentobarbital.

Sonomicrometry

Sonomicrometry is considered as the gold standard for assessment of myocardial deformation (function) in experimental studies.[74] The method uses small (2 mm in diameter) piezoelectric transducers ("crystals") that can both transmit and receive ultrasound signals (≥1 MHz). To perform a single distance measurement, one crystal will transmit a burst of ultrasound, and a second crystal will receive this ultrasound signal. The crystals are connected with a wire to a digital sonomicrometer and the elapsed time from transmission to reception is a direct and linear representation of the separation of the crystals. The resulting transit time is converted to a distance if the speed of sound in the material being measured is known (~1540 m/s in cardiac tissue). By repeating the measurement of transit-time hundreds of times per second, the instantaneous distance between crystals implanted in the myocardium can be assessed with high temporal resolution. Spatial resolution is determined by the distance between crystals. Because sonomicrometry involves implantation of foreign objects into the myocardium, it has been speculated that the method leads to injury and alters myocardial function. However,

studies using tissue-Doppler imaging have indicated that carefully implanted crystals have minimal effect on systolic or diastolic regional function.[75]

LV Rotation and Torsion by Sonomicrometry

For the estimation of LV rotation and torsion by sonomicrometry, 12 crystals were implanted in the LV in a grid-like manner to create 3 parallel short-axis planes (Figure 6). One crystal was implanted at the tip of the apex, and 11 crystals in the LV circumference at basal (n=3), equatorial (n=4) and apical (n=4) short-axis levels (Figure 6). Using the signals obtained from the 3-dimensional grid of crystals, the coordinates of each crystal were automatically determined by triangulation as a function of time. Parallel apical, equatorial and basal LV planes were constructed by interpolation of the corresponding crystal coordinates, and the in-plane positions were approximated by interpolation. The center of rotation for each LV plane was determined as the center of a best-fitted-circle through the interpolated coordinates. For each plane, the angular movements of the interpolated coordinates were averaged. Apical and basal rotation was calculated by measuring the difference in angular movement between the equatorial level (minimal rotation) and the apical and basal levels. LV torsion was estimated as the difference in angular movement between apical and basal planes at isochronal points (Figure 7).

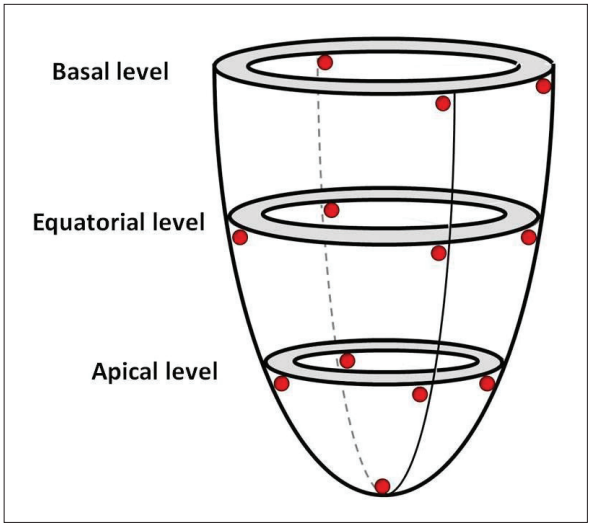

Figure 6. *A schematic representation of the LV with implanted sonomicro-metric crystals (filled circles) at the basal, equatorial and apical*

Echocardiographic Recordings

LV short-axis recordings were obtained using a Vivid 7 scanner (GE Vingmed). Transducer frequencies (1.7-2.0 MHz), sampling rates (60-110 frames per second), focus (mid-ventricular), sector depth (minimal) and sector width (narrow) were adjusted to optimize image quality. Short-axis echocardiograms were recorded in the same planes as used for sonomicrometry (basal, equatorial and apical), using the position of the crystals as reference. Echocardiographic recordings were done immediately before the sonomicrometry recordings.

Speckle Tracking Echocardiography

Speckle formation is a natural phenomenon which occurs when light or sound is scattered back from microrough surfaces. In echocardiography, a speckle pattern is the result of constructive and destructive interference of ultrasound backscattered from tissue structures smaller than a wavelength and the pattern is seen as characteristic intensity variations in an image. Although a speckle pattern is not a direct representation of the underlying tissue, its feature remains stable as long as the distances between scatters are unchanged. In echocardiography imaging, the distances between cardiac scatterers change constantly due to tissue deformation. However, given the high temporal resolution of modern scanners, the extent of myocardial deformation from one frame to the next is limited, resulting in moderate inter-frame degrading of a speckle pattern. Based on the assumption that speckle patterns are sufficiently preserved between frames and therefore represent myocardial “finger prints”, block-matching algorithms were developed for tracking local tissue motion from the displacement of speckle patterns visible in echocardiographic cine recordings. At the initiation of the experimental study (Paper I), no commercial STE software was available.

LV Rotation and Torsion by speckle tracking echocardiography

The speckle tracking algorithm used in the experimental study was originally developed by DrTech Hans Torp at NTNU for LV long-axis tracking, but in collaboration with DrIng Jonas Crosby, the algorithm was further modified for short-axis analyses. The algorithm, using minimum SAD (sum of absolute differences) of the B-mode pixel data,[76] was used to track the position of a kernel region (a selected region of interest (ROI) with a unique speckle pattern) frame by frame throughout the cardiac cycle. To avoid drifting, the tracking algorithm was applied both forward and backward, and the results were

averaged. Nine ROIs were automatically superimposed on the echo image at end-diastole and positioned to fit the circular shaped LV. In our experimental study this superimposed circle was aligned with the subepicardial LV circumference at the approximate same transmural level as the implanted crystals. Rotation was estimated as the average angular displacement of all ROIs relative to the center of a best fitted circle through the same ROIs, frame by frame. Torsion was estimated as the difference between apical and basal rotation at isochronal points (Figure 7).

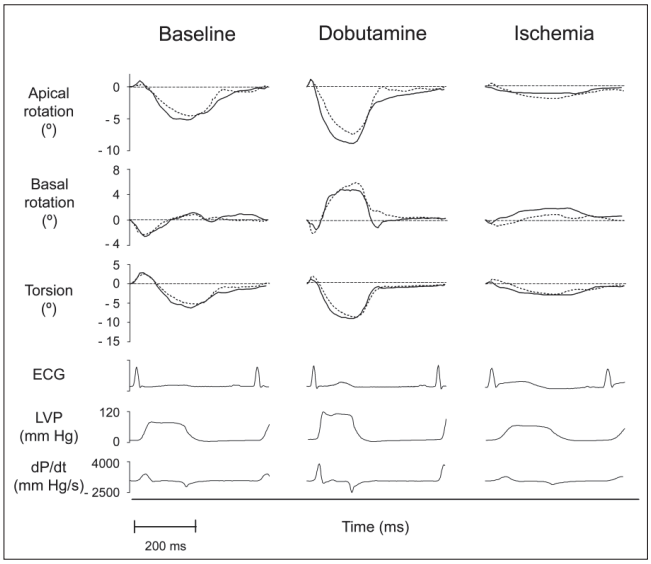

Figure 7. *Experimental study. Representative examples of apical and basal rotation and torsion at baseline, during dobutamine infusion and after 10 minutes of ischemia, as measured by sonomicrometry (dashed lines) and speckle tracking echocardiography (solid lines)*

Experimental Protocol

After baseline recordings, dobutamine was infused and recordings were repeated. After return of LV dP/dt to baseline values, the LAD was occluded for 10 minutes and recordings were obtained. Baseline data were obtained from 13 dogs, while dobutamine intervention was not performed in the first 4 experiments. In 5 dogs recordings during ischemia could not be obtained due to sustained ventricular fibrillation shortly after LAD-occlusion. In 6 dogs, STE short-axis recordings from multiple levels were obtained approximately 5 minutes before and 5 minutes after pericardiotomy to explore the importance of intact pericardium for LV rotation.

Magnetic Resonance Imaging (MRI)

MRI is considered as the reference method for assessment of cardiac anatomy, chamber volumes and function. The method is based on transmitting and receiving radio frequency signals from atomic nuclei spinning in a strong magnetic field. By adding weaker magnetic fields, MRI can generate cross-sectional 2-dimensional images in any plane. Due to its high spatial resolution, high signal-to-noise ratio and acceptable temporal resolution, MRI provides high-quality images of the LV. Myocardial tagging is a MRI technique that is considered as the reference method for quantification of regional LV function. By modulating the magnetization gradient, the signal from the myocardium can be nulled in a grid pattern prior to the onset of image acquisition. During imaging, the dark appearing grids move with the tissue and, thus, represent tissue markers. Areas of myocardium that are not contracting appropriately will demonstrate decreased grid deformation during the cardiac cycle. Intravenous contrast agents can be used to enhance the signal. Gadolinium chelates causes a shortening of T1 relaxation time, making gadolinium appear bright on T1-weighted images. In myocardial regions of infarction or fibrosis, gadolinium is retained for a longer period due to tissue damage and infarcted myocardium will therefore appear bright in images obtained 10-20 minutes after contrast injection (late enhancement).

MRI recordings

MRI scans were performed using 1.5 T scanners (Magnetom Vision Plus, Siemens, and Sigma CV/I, GE Medical Systems). Three long-axis and 8-10 short-axis cine loops covering the entire LV were obtained during breath hold (12-20 seconds) with a slice thickness of 7-10 mm and time resolution 35-40 ms. Multiple tagged short-axis recordings (8-10 slices) were obtained by prescribing parallel striped tags in 2 orthogonal orientations with a slice thickness of 7-10mm and a temporal resolution of 35-40 ms. Multiple late enhancement (LE) short-axis images (8-10 slices) with a thickness of ~10 mm were obtained 10-20 minutes after gadolinium injection.

LV rotation, torsion, strain, infarction and volume by MRI

LV rotation (Papers I-II), circumferential strain (Paper II) and radial strain (Paper III) by MRI tagging were analyzed by Harmonic Phase Imaging (HARP, version 1.0, Diagnosoft

Inc. Palo Alto, CA).[77] Myocardial infarct size by LE MRI was analyzed by PACS, Sectra, Sweden (Paper II) and by HARP (Paper III). LV volumes and EF (Paper III) were calculated by the true Simpson's method using QMass (Version 4.2, Medis, NL). LV torsion was calculated as the difference between apical and basal rotation at isochronal points. To ensure anatomical correspondence between short-axis recordings obtained by MRI and STE we used LV intracavitary diameter, wall thickness and anatomic landmarks. In Paper I, LV apical and basal rotation by MRI-tagging was calculated as the average of measurements obtained in the mid- and subendocardial layer to be consistent with measurements by STE. LV torsion was estimated as the difference between apical and basal rotation at isochronal points. In Paper II, LV apical rotation and strain by MRI and STE were compared according to a 4-segment model (in 3 patients, tagged MRI images could not be analyzed due to poor image quality). For comparison of LV apical infarct distribution by LE MRI and rotation and strain by STE, a detailed 36-segment LV model was used (12 segments for each of 3 short-axes). In Paper III, radial strain by MRI tagging was compared to measures by MDCT using an 18-segment LV model.

Echocardiographic recordings

In Papers I-II, using a Vivid 7 scanner (GE Vingmed Ultrasound, Horten, Norway), LV long- and short-axis recordings were obtained during breath holds with the individual in a supine left lateral position, within 5-15 minutes of the MRI examination. In order to obtain optimal speckle quality at reproducible and representative short-axis levels, projection of the LV base was obtained from a standard parasternal probe position, while projections of the LV apex, just proximal to the level with luminal closure at end-systole, was recorded from a anterior or anterolateral position, distal to the conventional parasternal apical window. An effort was made to make the LV cross-sections as circular as possible. Transducer frequencies (1.7-2.0 MHz), sampling rates (60-110 frames per second), focus (mid-ventricular), sector depth (minimal) and sector width (narrow) were adjusted to optimize image quality.

LV rotation and strain by STE

In Paper I we used the same Matlab-based software as in the experimental study. The analyses were performed in the same manner and the same criteria for adjustments or rejections of ROIs were used. However, in the clinical study the quality of the speckles improved progressively from the epi- to the endocardium and assessment of rotation was

therefore limited to the mid- and subendocardial layers. In Paper II LV apical rotation and circumferential strain were assessed using commercially available speckle tracking software (EchoPAC, GE Vingmed Ultrasound).[52] For each apical short-axis recording the endocardial border was manually traced in the frame where its complete contour was identified the best, and the automatically applied epicardial border was adjusted to cover the myocardium without including the pericardium. After successful tracking, rotation and strain were automatically calculated for numerous locations evenly distributed along the circumference and end-systolic rotation and strain were extracted from 24 evenly distributed segments that corresponded to the MRI segments.

Rotation and Strain in a Mathematical Simulation Model of the Ischemic LV

In Paper II we used the CMISS finite element analysis program (Bioengineering institute, University of Auckland, Auckland, New Zealand) to construct a finite element model to study mechanisms of changes in strain and rotation in the ischemic LV. The model included LV geometry, fiber-orientation, passive elastic myocardial properties, active systolic tension and stretch ratio along the fiber direction and time varying intracellular Ca^{2+} concentration.[78-80] According to a 12-segment apical short-axis model, an antero-septal infarct was included by abolishing active fiber force and increasing passive stiffness. Both transmural and non-transmural infarcts were simulated. The 3-dimensional deformation of the LV was simulated using physiological pressure-volume boundary conditions.

Multidetector Computer Tomography (MDCT)

MDCT has emerged as a noninvasive method for assessment of coronary anatomy and calcium burden, chamber volumes, wall motion, and myocardial scarring and perfusion. In MDCT, a two-dimensional array of detector elements replaces the linear array of detector elements used in typical conventional and helical CT scanners. The 2-dimensional detector array allows CT scanners to acquire multiple slices or sections simultaneously, which greatly increase the speed of CT image acquisition. A complete examination of the entire heart can be performed within seconds with excellent spatial resolution and signal-to-noise ratio and with acceptable temporal resolution and radiation dosage (4-6 mSv).[81]

MDCT recordings

In Paper III, retrospective ECG-gated MDCT images were obtained by a 64-slice scanner (Aquillion, Toshiba, Toshiba Medical Systems). Gantry rotation time was 400 ms to 500 ms depending on the heart rate and no beta-blocking agents were used. A bolus non-ionic contrast was administered and a navigation tool was used to obtain the highest possible temporal resolution. Two to 5 consecutive heart beats were used to reconstruct the R-R interval into ~20 phases and dedicated software (Vital Images, Minnetonka, Minnesota) was used to reformat the images into multiple long- and short-axis cine recordings. Image level-window was adjusted to optimize the contrast between tissue and blood and the recordings were stored in the AVI format for further analysis.

Multimodality tissue tracking (MTT)

The MTT algorithm is an automated pixel pattern-matching technique originally developed by Toshiba Medical Systems for STE.[54] However, in contrast to the speckle tracking algorithms used in Papers I-II, the MTT algorithm utilizes "on-screen" pixel information provided by cine loops stored in the DICOM or AVI format. By a template matching technique the motion of stable pixel patterns can be tracked frame by frame. Common determinants of accurate tracking include spatial resolution and signal-to-noise ratio. Because MDCT technology provides images of superb spatial resolution and high signal-to-noise ratio, the endo- and epicardial borders are well defined and their excursion in the radial direction suitable for automated tracking. By including the entire myocardial wall in the strain calculation, problems related to the transmural strain gradient are minimized.

Radial strain by MDCT

In LV basal, mid and apical short-axis MDCT cines, the endocardial and epicardial borders were drawn in an early-systolic frame, and the endocardial and epicardial displacement tracked throughout the cardiac cycle. After successful tracking, the magnitude and timing of peak systolic radial strain for each of 12 equiangular segments were extracted and used for further analyses. The RV inferior septal insertion point was used as reference for reproducible segmentation. Global end-systole was determined as the time of aortic valve closure. Strain values were not extracted from regions of inadequate tracking. We used a conventional 18-segment LV model (6 segments per short-axis) to compare radial strain by STE and MRI tagging, and a 36-segment LV

model (12 segments per short-axis) to compare radial strain mapping by MDCT and infarct extent by LE MRI (Figure 8).

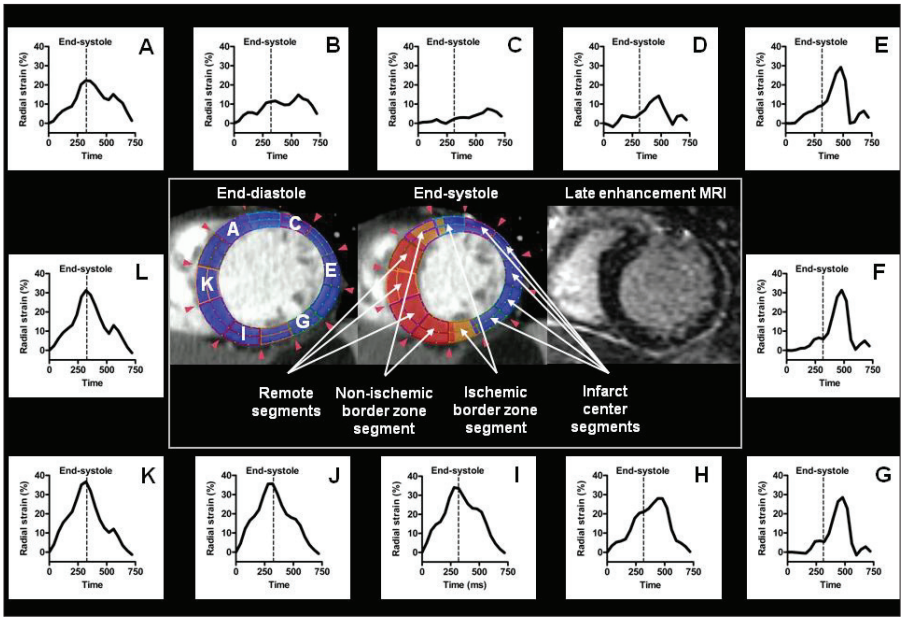

Figure 8. *Representative example of 12-segment radial strain analysis of the LV mid-ventricular short-axis by MTT MDCT in a patient with myocardial infarction of the anterior, lateral and posterior wall, as demonstrated by late enhancement MRI. While remote segments (J-L) demonstrate substantial wall thickening, infarct center segments (C-G) show severely impaired thickening. Note that ischemic border zone segments (B, H) show less thickening than non-ischemic border zone segments (A, I).*

Statistics

Values are expressed as mean±SD, unless otherwise stated. Statistical differences were considered significant at $P<0.05$. Variables from independent measurements were compared by a least square linear regression and by the Bland-Altman method (Papers I-III).[82] We used the unpaired t-test (Paper I) or one-way repeated-measures ANOVA followed by Bonferroni correction for predefined relevant comparisons (Papers I-II). In Paper III the linear mixed-model statistical method[83] with random intercept was used to assess the significance of infarct extent in explaining radial strain variations (SPSS 13 and 16, SPSS Inc., Chicago). Different relevant covariance structures were tested and the

analysis with lowest Akaike's Information Score selected. To determine inter- (Papers I-III) and intraobserver (Paper III) variability, recordings were randomly selected and independently analyzed. The reproducibility was expressed by the intraclass correlation coefficient and by the Bland-Altman method.

Summary of Results

Paper I

New Noninvasive Method for Assessment of Left Ventricular Rotation: Speckle Tracking Echocardiography

Background: Left ventricular (LV) torsion is due to oppositely directed apical and basal rotation and has been proposed as a sensitive marker of LV function. In the present study, we introduce and validate speckle tracking echocardiography (STE) as a method for assessment of LV rotation and torsion.

Methods: Apical and basal rotation by STE was measured from short-axis images by automatic frame-to-frame tracking of gray scale speckle patterns. Rotation was calculated as average angular displacement of 9 regions relative to the center of a best-fit circle through the same regions. As reference methods we used sonomicrometry in anesthetized dogs during baseline, dobutamine infusion, and apical ischemia, and magnetic resonance imaging (MRI) tagging in healthy humans.

Results: In dogs, the mean peak apical rotation was -3.7±1.2° (±SD) and -4.1±1.2°, and basal rotation 1.9±1.5° and 2.0±1.2° by sonomicrometry and STE, respectively. Rotations by both methods increased (P<0.001) during dobutamine infusion. Apical rotation by both methods decreased during left anterior descending coronary artery occlusion (P<0.007), whereas basal rotation was unchanged. In healthy humans, apical rotation was -11.6±3.8° and -10.9±3.3°, and basal rotation was 4.8±1.7° and 4.6±1.3° by MRI tagging and STE, respectively. Torsion measurement by STE showed good correlation and agreement with sonomicrometry (r= 0.94, p<0.001) and MRI (r=0.85, p<0.001).

Conclusions - The present study demonstrates that regional LV rotation and torsion can be measured accurately by STE, suggesting a new echocardiographic approach for quantification of LV systolic function.

Paper II

Clinical Assessment of Left Ventricular Rotation and Strain – A Novel Approach for Quantification of Function in Infarcted Myocardium and its Border Zones

Background: Left ventricular (LV) circumferential strain and rotation have been introduced as clinical markers of myocardial function. This study investigates how regional LV apical rotation and strain can be used in combination to assess function in the infarcted ventricle.

Methods: In healthy subjects (n = 15) and patients with myocardial infarction (n = 23), LV apical segmental rotation and strain were measured from apical short-axis recordings by speckle tracking echocardiography (STE) and MRI tagging. Infarct extent was determined by late gadolinium enhancement MRI. To investigate mechanisms of changes in strain and rotation, we used a mathematical finite element simulation model of the LV.

Results: Mean apical rotation and strain by STE were lower in patients than in healthy subjects (9.0 ± 4.9 vs. 12.9 ± 3.5° and -13.9 ± 10.7 vs. -23.8 ± 2.3%, respectively, $P < 0.05$). In patients, regional strain was reduced in proportion to segmental infarct extent ($r = 0.80$, $P < 0.0001$). Regional rotation, however, was similar in the center of the infarct and in remote viable myocardium. Minimum and maximum rotations were found at the infarct borders: minimum rotation at the border zone opposite to the direction of apical rotation, and maximum rotation at the border zone in the direction of rotation. The simulation model reproduced the clinical findings and indicated that the dissociation between rotation and strain was caused by mechanical interactions between infarcted and viable myocardium.

Conclusion: Systolic strain reflects regional myocardial function and infarct extent, whereas systolic rotation defines infarct borders in the LV apical region. Regional rotation, however, has limited ability to quantify regional myocardial dysfunction.

Paper III

Usefulness of Radial Strain Mapping by Multidetector Computer Tomography (MDCT) to Quantify Regional Myocardial Function in Patients with Healed Myocardial Infarction

Background: We introduce and evaluate strain mapping by multidetector computer tomography (MDCT) as a new non-invasive method for assessment of myocardial function. *Methods*: In patients (n=16) with healed myocardial infarction, peak systolic radial strain was measured by automated pixel pattern matching analysis of multiple left ventricular (LV) 64-slice MDCT short-axis recordings. For comparison, radial strain and myocardial infarct extent were measured by tagged magnetic resonance imaging (MRI) and late enhancement (LE) MRI, respectively.

Results: In a linear mixed model analysis, myocardial infarct extent was a strong predictor of segmental strain by MDCT (β=-0.44, P<0.0001). Strain was significantly different between non-infarcted (0%), non-transmurally (0-50%) and transmurally (>50%) infarcted segments (P<0.001), and between infarcted and non-infarcted border zone segments (P<0.001). There was a close relationship between strain by MDCT and by tagged MRI (r=0.68, P<0.0001 and mean difference -7.4±11.7%). Mean time-to-peak systolic strain was 324±42 by MDCT and 335±56 ms by tagged MRI (mean difference 11±40 ms).

Conclusion: To our knowledge this is the first study to demonstrate that regional myocardial function can be quantified by MDCT imaging, indicating that assessment of radial strain by MDCT might be a useful tool in the evaluation of patients with cardiovascular diseases.

Discussion

Accurate and reproducible assessment of LV function is pivotal for the majority of patients with cardiac diseases and is of particular importance in the setting of myocardial ischemia, the most common cause of LV dysfunction.[84] In the present thesis we have introduced and validated LV rotation and circumferential strain by STE and radial strain by multimodality tissue-tracking MDCT as new non-invasive methods for quantification of regional and global LV function. In Paper I we demonstrated that STE allows for quantitative assessment of LV rotation and torsion (Figure 9), indices that reflect fundamental properties of LV function. In an animal model, that allowed global and regional LV contractility to be altered, we showed that while LV torsion reflects global LV function, LV rotation is a more regional marker of LV function.

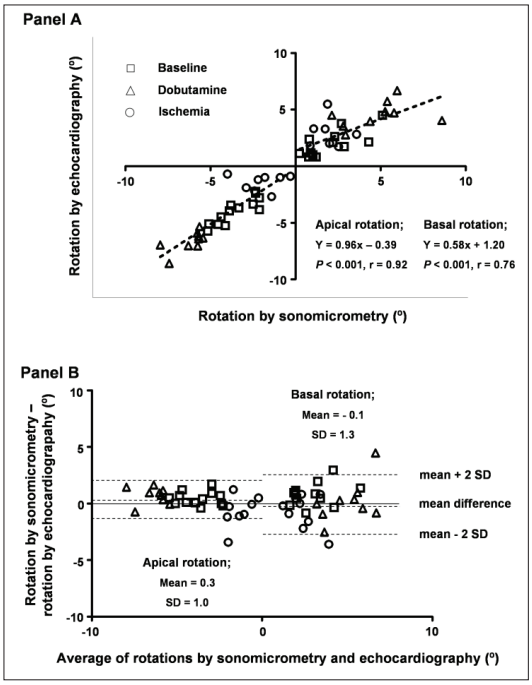

Figure 9. *Experimental data – rotation: A, correlation between rotation measured by sonomicrometry and STE. B, Agreement between rotation measured by sonomicrometry and STE.*

However, when analyzing the apical in-plane distribution of regional rotation and strain in a combined clinical and simulation study of the infarcted LV (Paper II), we observed that while a close association existed between regional circumferential strain and infarct transmurality, regional rotation did not provide a site-specific measure of regional

function, but defined infarct borders (Figure 10). The simulation model reproduced the clinical findings and supported our hypothesis that the dissociation between rotation and strain was caused by mechanical interactions between infarcted and viable myocardium.

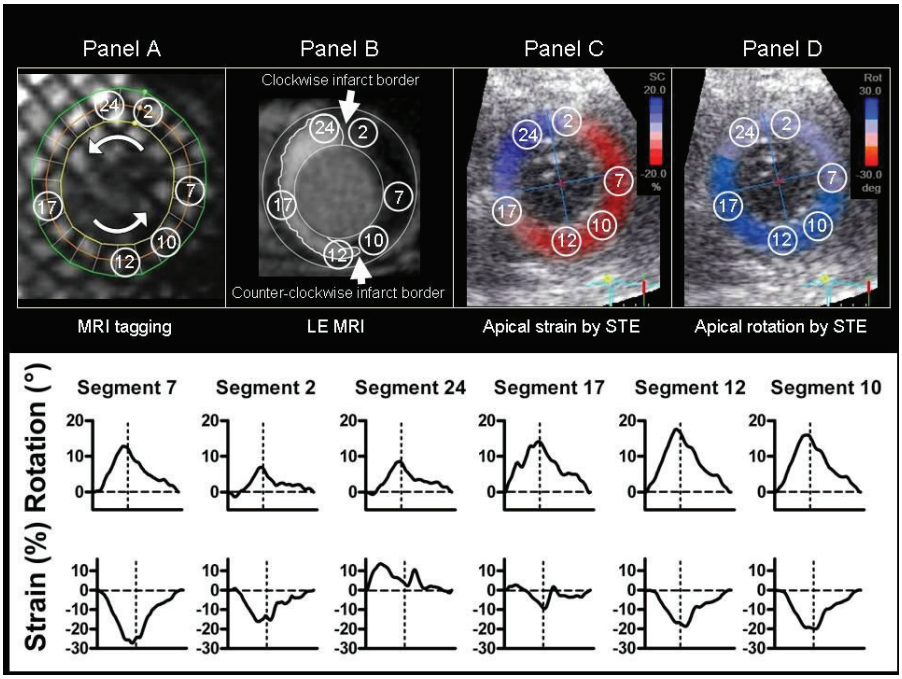

Figure 10. *Corresponding apical short-axis images by MRI tagging, late enhancement MRI and STE in a patient with LAD related myocardial infarction, demonstrating that while circumferential strain (bottom) reflects infarct transmurality, segments of maximum and minimum rotation reflect the two infarct borders (segments 2 and 12)*

Although echocardiography is the cornerstone for diagnosing and monitoring cardiac diseases, STE analysis is challenging in a significant number of patients due to insufficient image quality.[85] MDCT has rapidly emerged as a comprehensive, accurate and fast modality for assessment of cardiac and coronary anatomy, myocardial perfusion and scarring as well as volumes and wall motion. In Paper III we introduced and validated radial strain mapping by multimodality tissue tracking MDCT as a new method for quantification of global and regional LV function. In patients with healed myocardial infarction, the magnitude and timing of myocardial thickening was quantified in a highly detailed fashion by a novel automated pixel pattern matching technique from LV short-axis recordings by MDCT. The validity of our approach was confirmed by the use of

tagged MRI as a reference method. When the relationship between myocardial infarct extent and radial strain by MDCT was studied, significant differences in radial strain were observed between non-infarcted, non-transmurally infarcted and transmurally infarcted segments, and between infarcted and non-infarcted border zone segments (Figure 11). Furthermore, a significant correlation was observed between global LV radial strain and LV infarct size.

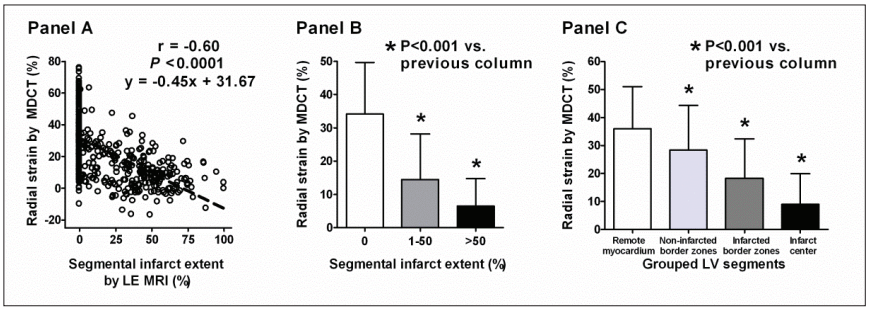

Figure 11. *A. Correlation between segmental infarct extent and radial strain by MDCT. B. Radial strain for non-infarcted, non-transmurally infarcted and transmurally infarcted segments. C. Radial strain for remote, border zone and infarct centre segments.*

Methodological considerations

Validation of LV Rotation, Torsion and Strain by STE

In Paper I, we demonstrated that LV basal and apical rotation and LV torsion could be measured non-invasively by automated tracking of speckles from echocardiographic LV short-axis recordings. The validity of our approach was tested using sonomicrometry as reference method in an animal model and MRI-tagging in humans. With sonomicrometry, the implanted myocardial crystals served as anatomic landmarks which ensured that the LV cross-sectional planes studied by the two methods were the same, and measurements could be done only a few seconds apart. Furthermore, in the animal model comparison between the methods could be done under a wide range of experimental settings known to alter LV rotation. The STE method showed dynamics, magnitudes and timing of peak basal and apical rotation and torsion that were closely related to measurements by sonomicrometry. The same relationship was found when STE was compared to MRI in healthy volunteers.

In Paper II, global and regional LV apical rotation and strain by STE was measured in healthy subjects and in patients with myocardial infarction using MRI-tagging as a reference method. Regional LV apical rotation and strain by STE demonstrated a close relationship to measures by MRI according to an apical 4-segment model. Because of limited spatial resolution of MRI tagging and impaired tag quality due to myocardial scarring, the 24-segment model used by STE could not be validated.

Two different STE algorithms were used in Papers I-II. At the time when the studies included in Paper I were initiated, no commercially speckle tracking software was available. We therefore used a Matlab-based algorithm developed by engineers at NTNU, Trondheim, Norway. The same software was used in the first validation study of strain by STE, published shortly after Paper I.[86] Just before onset of the study included in Paper II, commercially available software was introduced (EchoPAC, GE Vingmed) and given the obvious advantages of commonly available software, this was used in Paper II. To our knowledge, the two software have not been compared with respect to quantification of strain and rotation. However, because both algorithms use the block-matching approach, showed close relationship with their reference methods and demonstrated similar magnitude of global LV apical rotation in healthy subjects, there are good reasons to believe that the two algorithms are comparable.

Feasibility and reproducibility of STE analysis of mean LV basal and apical rotation (Paper I), and local LV apical rotation and strain (Paper II) were excellent (>90%). The typical time spent to complete a short-axis analysis, including adjustments and re-tracking if needed, was typically less than 60 seconds.

Validation of LV Strain by MDCT

To our knowledge, Paper III is the first study to demonstrate that regional myocardial function can be quantified in an automated and detailed fashion by MDCT imaging. Because MDCT technology provides images of high spatial resolution and high signal-to-noise ratio, the endo- and epicardial borders are well defined and their excursions suitable for automated feature tracking. In patients with healed myocardial infarction, the magnitude and timing of radial strain was quantified by a novel automated pixel pattern matching technique from MDCT LV short-axis recordings. The validity of our approach was tested by the use of tagged MRI as a reference method, and the magnitude and timing of radial strain by MDCT showed good correlation and agreement with measures by the

reference method. Radial strain by MDCT was measured with excellent intra- and inter-observer reproducibility.

Due to noise caused by ICD leads and motion artifacts, MDCT recordings could not be analyzed in 4 patients. Of the remaining studies, 97% of LV segments could be analyzed. The typical time spent to quantify regional strain from a LV short-axis MDCT cine by MTT was less than 60 seconds.

LV Rotation, Torsion and Strain by STE

LV Rotation and Torsion

In Paper I, LV rotation at the base was predominantly clockwise in both the experimental and clinical study, consistent with previous findings.[26, 33, 35, 36, 87-91] Dobutamine infusion caused a significant increase in clockwise rotation with no change in time to peak rotation. Apical ischemia caused no significant change in basal rotation reflecting that there was no impairment of LV function between equator and base. Some studies have indicated that basal LV rotation is minimal.[24, 25] However, in patients with aortic stenosis reduced magnitude of basal rotation compared to normals has been observed. Furthermore, in patients with chronic heart failure, 6 months of treatment was associated with an increase in basal rotation, while apical rotation was unchanged, indicating that measurement of basal rotation may be of clinical relevance. However, when compared to the reference methods, assessment of rotation by STE was less accurate for the basal level than for the apical level. Therefore, deviation in basal rotation may be difficult to assess by STE, and larger clinical studies have to be done in order to answer this question.

Counterclockwise rotation during LV ejection was demonstrated at the apical level in healthy individuals (Papers I-II) and was also found in the dog model. During dobutamine infusion there was an increase in apical rotation, and a tendency towards a decrease in time to peak rotation, whereas during LAD occlusion apical rotation was reduced. The same finding was observed in Paper II, where apical rotation was significantly lower in patients compared to healthy subjects. Changes in apical rotation by dobutamine and apical ischemia are in keeping with previous studies, using other methodologies.[30-32, 42, 45]

Although systolic apical rotation was predominantly counterclockwise, there was a small, clockwise rotation during isovolumic contraction. The oppositely directed rotation was demonstrated by both sonomicrometry and STE (Papers I-II) but not by MRI. This

phenomenon has been described previously and might be attributed to earlier activation of subendocardial fibers (right-handed helix) than subepicardial fibers.[37, 43, 92, 93] The reason why this motion was not recognized by MRI-tagging is probably the relatively low temporal resolution of the method (35 ms).

As demonstrated in Paper I, the LV apex and base showed, in principle, inversed rotational courses throughout the cardiac cycle. Because LV torsion is calculated as the rotational difference between apex and base at isochronal time points, and the magnitude of apical rotation far exceeds that of basal rotation, LV torsion is predominantly determined by apical rotation. This was demonstrated in the experimental study, where apical ischemia caused no change in basal rotation while both apical rotation and LV torsion were reduced. Furthermore, in a recent study by our group, using both experimental and clinical data, we showed that apical rotation represents the dominant contribution to LV torsion over a wide range of hemodynamic conditions, suggesting that apical rotation by STE may serve as a simple and feasible clinical index of LV torsion.[94]

Dissociation Between Regional Rotation and Strain

In Paper II, we demonstrated that regional LV apical rotation and strain reflect entirely different features of infarcted myocardium. Reductions in end-systolic strain in post-infarct patients corresponded to transmural extent of infarcted myocardium, as evidenced by a strong correlation between systolic strain and percent infarction within segments. These observations were in keeping with previous studies and confirmed that systolic strain reflects regional contractile function.[60, 95-98] This was in contrast to regional rotation which did not reflect regional contractility. Maximum and minimum values of regional rotation, however, were markers of the anatomical locations of the infarct borders. The simulation study reproduced the clinical findings and provided insights into the mechanism of the apparent inconsistency between regional apical rotation and strain: While oblique LV fibers running from the base to the apex account for the overall counter-clockwise rotation of the apex, the circumferential fibers affect the in-plane distribution of regional rotation, which in the normal LV is homogeneous. Due to the imbalance of circumferentially oriented contractile forces in the setting of regional ischemia, the ischemic myocardium will be pulled from both sides by non-infarcted myocardium. Consequently, the counter-clockwise infarct border is pulled in the counter-clockwise direction (same direction as overall apical rotation) while the clockwise infarct border is pulled in the opposite, clockwise direction. In total, these mechanisms cause

hyper-rotation of the counter-clockwise border zone, and hypo-rotation of the clockwise border zone (Figure 12).

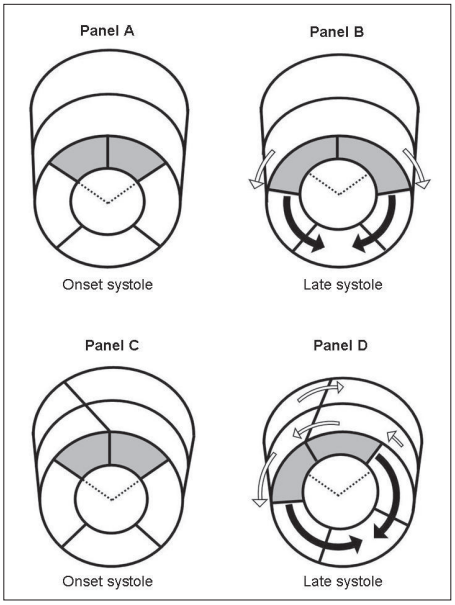

Figure 12. *Schematic representations of the LV viewed from the apex towards the base. Ischemic myocardium (gray area), direction of rotation (open arrows), circumferential forces acting on the ischemic region (solid arrows) and ischemic margins at onset of systole (dotted lines) are indicated. Upper panels illustrate rotational deformation of an apical short-axis slice in an LV consisting of circumferential fibers only. Lower panels illustrate rotational deformation of an apical short-axis slice in an LV consisting of circumferential and oblique myocardial fibers. Open arrow length indicates mangitude of rotation.*

Comparison with previous studies

Rotation and Torsion in the Normal LV

The magnitudes of LV apical and basal rotation and torsion, as reported in previous experimental and clinical studies, differ substantially, and a number of factors may explain this variance.[23-27, 32, 33, 35-37, 40, 42, 44-47, 47, 87, 88, 91, 99-102] As demonstrated by Henson et al.[103] apparent differences in torsion between mice and humans are due to different sizes of their ventricles. When systolic torsion angle was normalized for LV length, torsion was essentially similar in the two species. Furthermore, since torsion angle is a non-linear function of ventricular length, its magnitude depends critically on measurement level relative to the LV base or other reference points. The relatively high values of apical rotation measured by Gibbons Kroeker et al.[24] is most likely explained by their measurement technique, which recorded rotation at the distal part of the LV apex. Another factor that may explain some of the variance in torsion magnitude in different

studies is the existence of a marked transmural gradient with subendocardial values almost twice the subepicardial.[23] In the dog model we measured subepicardial rotation, and during baseline conditions torsion was approximately 6º. These values are in the same range as was reported by Buchalter et al,[32] who measured both subepicardial and subendocardial torsion in anesthetized dogs by MRI tagging. Furthermore, the hemodynamic and contractile status of the heart in different animal models may vary and give rise to differences in torsion. In our study, a significant reduction in rotation at the apical level and a trend towards a reduction at the base was observed during the 2- to 3-hour period before the baseline recordings. This was associated with reductions in LVP and LV dP/dt_{max}, indicating that there was some reduction in LV systolic function. Most likely the decrease in rotation reflects impairment of LV function due to the extensive surgical instrumentation.

LV Rotation and Strain in the Ischemic LV

Several studies have confirmed that ischemia reduces LV rotation, but no studies have investigated the interaction between regional shortening and rotation in the ischemic ventricle. In an experimental MRI tagging study by Buchalter et al the relationship between distribution of LV torsion and ischemia was examined.[32] Local torsion was measured as the rotational difference between corresponding apical and basal locations before and during LAD-occlusion. Local torsion was further grouped into 2 LV sections, an anterior and a posterior, only the former showing reduced torsion during ischemia. Because LAD-occlusion primarily affects the anterior LV wall, the observations made by Buchalter et al. of reduced torsion of the anterior section during ischemia, can be interpreted as inconsistent with our results. However, according to the depiction of the distribution of apical ischemia in each animal in their study, the anterior and posterior sections did not represent strictly ischemic and non-ischemic myocardium, respectively: In all animals the lateral *non-ischemic* border-zone, which in our study represents myocardium of *hypo-rotation*, was located in the *anterior* ("ischemic") section, while the septal *ischemic* border-zone, which in our study represents myocardium of *hyper-rotation* was located in the *posterior* ("non-ischemic") section. Consequently, the apparent discrepancies between our observations and the findings by Buchalter et al, could be explained by their inclusion of non-ischemic myocardium of hypo-rotation in the anterior LV section, and ischemic myocardium of hyper-rotation in the posterior LV section.

Radial strain by MDCT

The clinical use of MDCT for assessment of cardiac anatomy, coronary angiography and myocardial perfusion is rapidly increasing. By acquiring retrospective ECG-gated data, cine loops can also be constructed from the same dataset. Conventional non-invasive LV strain analysis uses 3 short-axis slices to construct a 16-segment model.[104] Given the heterogeneous distribution of myocardial infarct transmurality[64, 69, 70] and the high quality of MDCT images, in Paper III we used a 36-segment LV model to obtain a more detailed mapping of the relationship between myocardial deformation and infarct morphology. The construction of narrower segments ensured that each category contained morphologically more homogeneous segment and reduced the likelihood of including "contaminated" segments, particularly in the non-infarcted and infarcted border zone groups. In our study, the close inverse relationship observed between radial strain and infarct transmurality allowed for discrimination between segments of various infarct transmurality and between infarcted and non-infarcted border zone segments. These observations were in keeping with the STE data presented in Paper II regarding circumferential strain mapping.

Although sonomicrometry studies have demonstrated that the three strain components respond equally to acute ischemia, controversies exist regarding the sensitivity of the various strain components in the setting of chronic infarction. A strong inverse relationship between infarct transmurality and strain has consistently been demonstrated in the circumferential or longitudinal directions, while conflicting reports exist regarding the sensitivity of radial strain.[67, 96, 105-111] A possible explanation for this inconsistency relates to methodological issues, as radial strain has been the most challenging strain component to measure non-invasively, showing greater variability and less reproducibility when compared to assessment of circumferential or longitudinal strain.[67, 96, 110, 112] Current strain imaging methods utilize intramyocardial markers for tissue tracking. Because radial strain increases by almost 100% when moving from the subepicardium towards the subendocardium, the magnitude of radial strain measurements strongly depends on the transmural location of the myocardial markers used for tracking.[111, 113-116] Consequently, given the limited number of MR tags across the LV wall and the reduction in speckle quality in echocardiographic images when moving towards the subepicardium, radial strain imaging by these techniques is challenging.[87] In this perspective, the introduction of radial strain by MDCT is an important supplement to

strain analyses by other modalities. Furthermore, recent patient studies of cardiac resynchronization therapy have indicated that radial strain may characterize LV mechanical dyssynchrony in a more sensitive manner than longitudinal strain, further supporting the relevance of radial strain measurements by MDCT.[117, 118]

Limitations

Material

The number of study subjects included in Papers I-III was relatively small. The healthy subjects in Papers I-II were relatively young and patients included in Paper II had mostly LAD-related infarctions. In Paper III, no subjects with preserved LV function were included. Consequently, to determine the clinical applicability of our findings, larger studies are need that should include older subjects and patients with a wider range of myocardial dysfunction and infarct localizations.

Sonomicrometry

A limitation with the sonomicrometry model was the lack of extra-cardiac reference for the crystal positions, which represented a fundamental difference between STE and sonomicrometry. While STE provided a measure relative to a fixed reference point outside the heart (the echocardiography transducer), in our model sonomicrometry had no such external reference. Therefore, sonomicrometry provided no direct measure of rotation. To compensate for this limitation we used the LV equatorial plane, which has essentially zero rotation, as reference plane. This assumption is justified by a number of previous studies in different species, including dogs, that show only minimal rotation at the LV equator,[26, 35, 36, 87, 90, 91, 103] and was supported by the observation in the present study that rotation at the equatorial level by STE was minimal. For assessment of torsion, however, the difference between apical and basal rotation, no assumptions about the equatorial plane was needed.

Speckle tracking echocardiography

Several important factors may influence the accuracy of speckle tracking. The quality of the recordings must be high in order to achieve correct tracking, and requires proper adjustment of frame rate, probe frequency and focus. In Paper I, tracking quality was evaluated visually and individual ROIs of poor tracking were manually moved to areas of

better speckle quality, or deleted. Since rotational displacement is relatively homogenously distributed around the LV circumference in healthy myocardium, deletion of one or maximum two ROIs will have minimal effect on the average rotation.[23, 32, 46] In Paper II, using commercially available software, inadequate tracking was also visually evaluated and the endocardial delineation manually adjusted in regions of poor tracking or drawn in another frame until better tracking was achieved. In this study, only apical short-axes were analyzed and no regions had to be excluded.

A fundamental problem with speckle tracking in LV short-axis images is that longitudinal motion of the LV causes myocardium to move in and out of the image plane. As a consequence, speckles generated from the ultrasound beam (2-3mm of thickness) will represent myocardium from different cross-sectional levels during the cardiac cycle. The experimental study (Paper I) demonstrated that this problem was most pronounced at the LV base where the longitudinal displacement was approximately 4 mm from ED to ES, while LV apex was essentially stationary. The fact that the relationship between STE and the reference methods was best at the apical level might well be attributed to this phenomenon, further supported by the successful tracking of all apical segments in Paper II.

A limitation in the clinical studies was that speckle quality in some cases was suboptimal in the subepicardial layer of the LV. Therefore, for the validation of LV rotation against MRI in Paper I, we compared measurements from the mid and inner wall layers. In Paper II, a different tracking algorithm was used, and the automatically applied epicardial delineation was adjusted to cover the myocardium without including the epicardium. Hopefully technical developments in the ultrasound technology will resolve the problem with suboptimal subepicardial speckle quality. In the dog study we had direct access to the heart via a sternotomy and by using ultrasound gel as standoff we obtained satisfactory tracking quality in all layers of the LV wall.

One limitation for the clinical routine use of STE is the selection of reproducible anatomical landmarks for measuring apical rotation. One approach is to move the cross-sectional image plane as far distally as possible. Another approach could be to measure at the most distal level that does not have luminal closure during systole. At the basal level, reproducible image planes were easier to obtain, using the fibrous mitral ring for orientation. Selection of imaging plane is a challenge and clinical testing of STE in patients are needed to determine if reproducible measures can be obtained from ventricles

that may change in size and geometry over time. Also, given the recent advances in 3-dimensional echocardiography imaging, it is likely that this problem will be solved.

Given the mechanical complexity of 3-dimensional myocardial deformation and interaction, in Paper II a more complete approach would have been to include measures of regional shear strain and torsion in our analysis. In principle such measures can be estimated by combining analyses from multiple 2-dimensional cross-sectional recordings. However, by current echocardiographic techniques this method is challenging, particularly with respect to determining the distance between slices and to our approach of detailed strain- and rotation mapping. Hopefully, 3-dimensional echocardiography imaging will allow simultaneous calculation of regional rotation, strain, shear strain and torsion in the near future.

MRI tagging

Although strain by tagged MRI is considered as the reference method for non-invasive quantification of myocardial function, strain analysis in the infarcted LV may be challenging due to suboptimal tag lines within fibrotic tissue. Assessment of strain in the radial direction is further challenged by signal-to-noise limitations in most 1.5 T MRI systems, which only allow one or two tag planes to be inserted between the endo and epicardium,[87] and by post-infarct wall thinning in transmurally infarcted segments.

MDCT

Due to the radiation involved in MDCT imaging, the inclusion of patients must be carefully weighed and subjects with preserved LV function are therefore currently not likely to undergo protocols needed for cine construction. In our study, mean radiation dose was 10.8±2.4 mSv, which is similar to the effective radiation doses in abdominal CT (10 mSv), but more than in a diagnostic catheterization (7 mSv).[81] Although the feasibility of MTT analysis of subjects with preserved LV function has not been proven, a substantial number of remote segments demonstrated radial strain values similar to those previously reported in healthy subjects, indicates that adequate tracking is feasible also in the healthy LV. Finally, the use of a 64-slice MDCT scanner in our study in part limited the temporal and spatial resolution of our cine recordings.

Conclusions

In the present thesis we have demonstrated that

- the magnitude and timing of apical and basal LV rotation and torsion can be measured accurately by STE;
- a close association exists between regional circumferential strain and infarct transmurality and between locations of maximum and minimum rotation and infarct borders;
- the magnitude and timing of LV radial strain can be measured accurately by MDCT;
- when analyzed in a detailed fashion, a close association exists between the distribution of radial strain and infarct transmurality.

These findings indicate that assessment of rotation and circumferential strain by STE and radial strain by MDCT may have potentials to become clinical noninvasive tools for detection and quantification of LV ischemia.

Reference List

1. Cohn JN, Duprez DA. Time to foster a rational approach to preventing cardiovascular morbid events. *J Am Coll Cardiol.* 2008;52:327-329.

2. Fraser AG, Buser PT, Bax JJ, Dassen WR, Nihoyannopoulos P, Schwitter J, Knuuti JM, Hoher M, Bengel F, Szatmari A. The future of cardiovascular imaging and non-invasive diagnosis: a joint statement from the European Association of Echocardiography, the Working Groups on Cardiovascular Magnetic Resonance, Computers in Cardiology, and Nuclear Cardiology, of the European Society of Cardiology, the European Association of Nuclear Medicine, and the Association for European Paediatric Cardiology. *Eur Heart J.* 2006;27:1750-1753.

3. Howard BV, Rodriguez BL, Bennett PH, Harris MI, Hamman R, Kuller LH, Pearson TA, Wylie-Rosett J. Prevention Conference VI: Diabetes and Cardiovascular disease: Writing Group I: epidemiology. *Circulation.* 2002;105:e132-e137.

4. Voelkel NF, Quaife RA, Leinwand LA, Barst RJ, McGoon MD, Meldrum DR, Dupuis J, Long CS, Rubin LJ, Smart FW, Suzuki YJ, Gladwin M, Denholm EM, Gail DB. Right ventricular function and failure: report of a National Heart, Lung, and Blood Institute working group on cellular and molecular mechanisms of right heart failure. *Circulation.* 2006;114:1883-1891.

5. D'hooge J, Heimdal A, Jamal F, Kukulski T, Bijnens B, Rademakers F, Hatle L, Suetens P, Sutherland GR. Regional strain and strain rate measurements by cardiac ultrasound: principles, implementation and limitations. *Eur J Echocardiogr.* 2000;1:154-170.

6. Mahnken AH, Koos R, Katoh M, Spuentrup E, Busch P, Wildberger JE, Kuhl HP, Gunther RW. Sixteen-slice spiral CT versus MR imaging for the assessment of left ventricular function in acute myocardial infarction. *Eur Radiol.* 2005;15:714-720.

7. Sibley CT, Lima JA. Assessment of ventricular structure and function with multidetector CT and MRI. *Curr Cardiol Rep.* 2008;10:67-71.

8. Butler J, Shapiro MD, Jassal DS, Neilan TG, Nichols J, Ferencik M, Brady TJ, Hoffmann U, Cury RC. Comparison of multidetector computed tomography and two-dimensional transthoracic echocardiography for left ventricular assessment in patients with heart failure. *Am J Cardiol.* 2007;99:247-249.

9. Cury RC, Nieman K, Shapiro MD, Butler J, Nomura CH, Ferencik M, Hoffmann U, Abbara S, Jassal DS, Yasuda T, Gold HK, Jang IK, Brady TJ. Comprehensive assessment of myocardial perfusion defects, regional wall motion, and left ventricular function by using 64-section multidetector CT. *Radiology.* 2008;248:466-475.

10. Sabarudin A, Sun Z, Ng KH. A systematic review of radiation dose associated with different generations of multidetector CT coronary angiography. *J Med Imaging Radiat Oncol.* 2012;56:5-17.

11. Carabello BA, Nolan SP, McGuire LB. Assessment of preoperative left ventricular function in patients with mitral regurgitation: value of the end-systolic wall stress-end-systolic volume ratio. *Circulation.* 1981;64:1212-1217.

12. Gunther S, Grossman W. Determinants of ventricular function in pressure-overload hypertrophy in man. *Circulation.* 1979;59:679-688.

13. Malm S, Frigstad S, Sagberg E, Larsson H, Skjaerpe T. Accurate and reproducible measurement of left ventricular volume and ejection fraction by contrast echocardiography: a comparison with magnetic resonance imaging. *J Am Coll Cardiol.* 2004;44:1030-1035.

14. Marciniak A, Claus P, Sutherland GR, Marciniak M, Karu T, Baltabaeva A, Merli E, Bijnens B, Jahangiri M. Changes in systolic left ventricular function in isolated mitral regurgitation. A strain rate imaging study. *Eur Heart J.* 2007;28:2627-2636.

15. Cucchini F, Baldi G, Barilli AL, Di Donato M, Visioli O. Tardokinesis in coronary artery disease: evidence with instantaneous analysis of left ventricular ejection. *Eur J Cardiol.* 1981;12:153-166.

16. Ehring T, Heusch G. Left ventricular asynchrony: an indicator of regional myocardial dysfunction. *Am Heart J.* 1990;120:1047-1057.

17. Guth BD, Schulz R, Heusch G. Time course and mechanisms of contractile dysfunction during acute myocardial ischemia. *Circulation.* 1993;87:IV35-IV42.

18. Mirsky I, Parmley WW. Assessment of passive elastic stiffness for isolated heart muscle and the intact heart. *Circ Res.* 1973;33:233-243.

19. Bugge-Asperheim B, Lekven J, Kiil F. Effect of saline infusion on stroke volume and end-systolic volume at various levels of adrenergic activity in dogs. *Scand J Clin Lab Invest.* 1972;29:15-24.

20. Zerhouni EA, Parish DM, Rogers WJ, Yang A, Shapiro EP. Human heart: tagging with MR imaging--a method for noninvasive assessment of myocardial motion. *Radiology.* 1988;169:59-63.

21. Urheim S, Edvardsen T, Torp H, Angelsen B, Smiseth OA. Myocardial strain by Doppler echocardiography. Validation of a new method to quantify regional myocardial function. *Circulation.* 2000;102:1158-1164.

22. Sengupta PP, Tajik AJ, Chandrasekaran K, Khandheria BK. Twist mechanics of the left ventricle: principles and application. *JACC Cardiovasc Imaging.* 2008;1:366-376.

23. Buchalter MB, Weiss JL, Rogers WJ, Zerhouni EA, Weisfeldt ML, Beyar R, Shapiro EP. Noninvasive quantification of left ventricular rotational deformation in normal humans using magnetic resonance imaging myocardial tagging. *Circulation.* 1990;81:1236-1244.

24. Gibbons Kroeker CA, Ter Keurs HE, Knudtson ML, Tyberg JV, Beyar R. An optical device to measure the dynamics of apex rotation of the left ventricle. *Am J Physiol Heart Circ Physiol.* 1993;265:H1444-H1449.

25. Knudtson ML, Galbraith PD, Hildebrand KL, Tyberg JV, Beyar R. Dynamics of left ventricular apex rotation during angioplasty: a sensitive index of ischemic dysfunction. *Circulation.* 1997;96:801-808.

26. Nichols K, Kamran M, Cooke CD, Faber TL, Garcia EV, Bergmann SR, Depuey EG. Feasibility of detecting cardiac torsion in myocardial perfusion gated SPECT data. *J Nucl Cardiol.* 2002;9:500-507.

27. Mirro MJ, Rogers EW, Weyman AE, Feigenbaum H. Angular displacement of the papillary muscles during the cardiac cycle. *Circulation.* 1979;60:327-333.

28. Beyar R, Yin FC, Hausknecht M, Weisfeldt ML, Kass DA. Dependence of left ventricular twist-radial shortening relations on cardiac cycle phase. *Am J Physiol.* 1989;257:H1119-H1126.

29. Ingels NB, Jr., Daughters GT, Stinson EB, Alderman EL. Measurement of midwall myocardial dynamics in intact man by radiography of surgically implanted markers. *Circulation.* 1975;52:859-867.

30. Gibbons Kroeker CA, Tyberg JV, Beyar R. Effects of load manipulations, heart rate, and contractility on left ventricular apical rotation. An experimental study in anesthetized dogs. *Circulation.* 1995;92:130-141.

31. Kroeker CA, Tyberg JV, Beyar R. Effects of ischemia on left ventricular apex rotation. An experimental study in anesthetized dogs. *Circulation.* 1995;92:3539-3548.

32. Buchalter MB, Rademakers FE, Weiss JL, Rogers WJ, Weisfeldt ML, Shapiro EP. Rotational deformation of the canine left ventricle measured by magnetic resonance tagging: effects of catecholamines, ischaemia, and pacing. *Cardiovasc Res.* 1994;28:629-635.

33. Fuchs E, Muller MF, Oswald H, Thony H, Mohacsi P, Hess OM. Cardiac rotation and relaxation in patients with chronic heart failure. *Eur J Heart Fail.* 2004;6:715-722.

34. Maier SE, Fischer SE, McKinnon GC, Hess OM, Krayenbuehl HP, Boesiger P. Evaluation of left ventricular segmental wall motion in hypertrophic cardiomyopathy with myocardial tagging. *Circulation.* 1992;86:1919-1928.

35. Nagel E, Stuber M, Lakatos M, Scheidegger MB, Boesiger P, Hess OM. Cardiac rotation and relaxation after anterolateral myocardial infarction. *Coron Artery Dis.* 2000;11:261-267.

36. Sandstede JJ, Johnson T, Harre K, Beer M, Hofmann S, Pabst T, Kenn W, Voelker W, Neubauer S, Hahn D. Cardiac systolic rotation and contraction before and after valve replacement for aortic stenosis: a myocardial tagging study using MR imaging. *AJR Am J Roentgenol.* 2002;178:953-958.

37. Yun KL, Niczyporuk MA, Daughters GT, Ingels NB, Jr., Stinson EB, Alderman EL, Hansen DE, Miller DC. Alterations in left ventricular diastolic twist mechanics during acute human cardiac allograft rejection. *Circulation.* 1991;83:962-973.

38. DeAnda A, Jr., Komeda M, Nikolic SD, Daughters GT, Ingels NB, Miller DC. Left ventricular function, twist, and recoil after mitral valve replacement. *Circulation.* 1995;92:II458-II466.

39. Hansen DE, Daughters GT, Alderman EL, Ingels NB, Stinson EB, Miller DC. Effect of volume loading, pressure loading, and inotropic stimulation on left ventricular torsion in humans. *Circulation.* 1991;83:1315-1326.

40. Tibayan FA, Rodriguez F, Langer F, Zasio MK, Bailey L, Liang D, Daughters GT, Ingels NB, Jr., Miller DC. Alterations in left ventricular torsion and diastolic recoil after myocardial infarction with and without chronic ischemic mitral regurgitation. *Circulation.* 2004;110:II109-II114.

41. Sorger JM, Wyman BT, Faris OP, Hunter WC, McVeigh ER. Torsion of the left ventricle during pacing with MRI tagging. *J Cardiovasc Magn Reson.* 2003;5:521-530.

42. Rademakers FE, Buchalter MB, Rogers WJ, Zerhouni EA, Weisfeldt ML, Weiss JL, Shapiro EP. Dissociation between left ventricular untwisting and filling. Accentuation by catecholamines. *Circulation.* 1992;85:1572-1581.

43. McDonald IG. The shape and movements of the human left ventricle during systole. A study by cineangiography and by cineradiography of epicardial markers. *Am J Cardiol.* 1970;26:221-230.

44. Moon MR, Ingels NB, Jr., Daughters GT, Stinson EB, Hansen DE, Miller DC. Alterations in left ventricular twist mechanics with inotropic stimulation and volume loading in human subjects. *Circulation.* 1994;89:142-150.

45. Dong SJ, Hees PS, Huang WM, Buffer SA, Jr., Weiss JL, Shapiro EP. Independent effects of preload, afterload, and contractility on left ventricular torsion. *Am J Physiol.* 1999;277:H1053-H1060.

46. Hansen DE, Daughters GT, Alderman EL, Ingels NB, Jr., Miller DC. Torsional deformation of the left ventricular midwall in human hearts with intramyocardial markers: regional heterogeneity and sensitivity to the inotropic effects of abrupt rate changes. *Circ Res.* 1988;62:941-952.

47. DeAnda A, Jr., Moon MR, Yun KL, Daughters GT, Ingels NB, Jr., Miller DC. Left ventricular torsional dynamics immediately after mitral valve replacement. *Circulation.* 1994;90:II339-II346.

48. Delhaas T, Kotte J, van der Toorn A, Snoep G, Prinzen FW, Arts T. Increase in left ventricular torsion-to-shortening ratio in children with valvular aortic stenosis. *Magn Reson Med.* 2004;51:135-139.

49. MacGowan GA, Burkhoff D, Rogers WJ, Salvador D, Azhari H, Hees PS, Zweier JL, Halperin HR, Siu CO, Lima JA, Weiss JL, Shapiro EP. Effects of afterload on regional left ventricular torsion. *Cardiovasc Res.* 1996;31:917-925.

50. Moon MR, DeAnda A, Jr., Daughters GT, Ingels NB, Miller DC. Effects of chordal disruption on regional left ventricular torsional deformation. *Circulation.* 1996;94:II143-II151.

51. Tischler M, Niggel J. Left ventricular systolic torsion and exercise in normal hearts. *J Am Soc Echocardiogr.* 2003;16:670-674.

52. Leitman M, Lysyansky P, Sidenko S, Shir V, Peleg E, Binenbaum M, Kaluski E, Krakover R, Vered Z. Two-dimensional strain-a novel software for real-time quantitative echocardiographic assessment of myocardial function. *J Am Soc Echocardiogr.* 2004;17:1021-1029.

53. Reisner SA, Lysyansky P, Agmon Y, Mutlak D, Lessick J, Friedman Z. Global longitudinal strain: a novel index of left ventricular systolic function. *J Am Soc Echocardiogr.* 2004;17:630-633.

54. Ogawa K, Hozumi T, Sugioka K, Matsumura Y, Nishiura M, Kanda R, Abe Y, Takemoto Y, Yoshiyama M, Yoshikawa J. Usefulness of automated quantitation of regional left ventricular wall motion by a novel method of two-dimensional echocardiographic tracking. *Am J Cardiol.* 2006;98:1531-1537.

55. Kwong RY, Chan AK, Brown KA, Chan CW, Reynolds HG, Tsang S, Davis RB. Impact of unrecognized myocardial scar detected by cardiac magnetic resonance imaging on event-free survival in patients presenting with signs or symptoms of coronary artery disease. *Circulation.* 2006;113:2733-2743.

56. Kim RJ, Wu E, Rafael A, Chen EL, Parker MA, Simonetti O, Klocke FJ, Bonow RO, Judd RM. The use of contrast-enhanced magnetic resonance imaging to identify reversible myocardial dysfunction. *N Engl J Med.* 2000;343:1445-1453.

57. Orn S, Manhenke C, Anand IS, Squire I, Nagel E, Edvardsen T, Dickstein K. Effect of left ventricular scar size, location, and transmurality on left ventricular remodeling with healed myocardial infarction. *Am J Cardiol.* 2007;99:1109-1114.

58. Tarantini G, Razzolini R, Cacciavillani L, Bilato C, Sarais C, Corbetti F, Marra MP, Napodano M, Ramondo A, Iliceto S. Influence of transmurality, infarct size, and severe microvascular obstruction on left ventricular remodeling and function after primary coronary angioplasty. *Am J Cardiol.* 2006;98:1033-1040.

59. Choi KM, Kim RJ, Gubernikoff G, Vargas JD, Parker M, Judd RM. Transmural extent of acute myocardial infarction predicts long-term improvement in contractile function. *Circulation.* 2001;104:1101-1107.

60. Gerber BL, Garot J, Bluemke DA, Wu KC, Lima JA. Accuracy of contrast-enhanced magnetic resonance imaging in predicting improvement of regional myocardial function in patients after acute myocardial infarction. *Circulation.* 2002;106:1083-1089.

61. Yan AT, Shayne AJ, Brown KA, Gupta SN, Chan CW, Luu TM, Di Carli MF, Reynolds HG, Stevenson WG, Kwong RY. Characterization of the peri-infarct zone by contrast-enhanced cardiac magnetic resonance imaging is a powerful predictor of post-myocardial infarction mortality. *Circulation.* 2006;114:32-39.

62. Gibbons RJ, Valeti US, Araoz PA, Jaffe AS. The quantification of infarct size. *J Am Coll Cardiol.* 2004;44:1533-1542.

63. Tennant R, Wiggers CJ. The effect of coronary occlusion on myocardial contraction. *Am J Physiol.* 1935;112:351-361.

64. Reimer KA, Lowe JE, Rasmussen MM, Jennings RB. The wavefront phenomenon of ischemic cell death. 1. Myocardial infarct size vs duration of coronary occlusion in dogs. *Circulation.* 1977;56:786-794.

65. Reimer KA, Jennings RB. The "wavefront phenomenon" of myocardial ischemic cell death. II. Transmural progression of necrosis within the framework of ischemic bed size (myocardium at risk) and collateral flow. *Lab Invest.* 1979;40:633-644.

66. Pierard LA, Albert A, Chapelle JP, Carlier J, Kulbertus HE. Relative prognostic value of clinical, biochemical, echocardiographic and haemodynamic variables in predicting in-hospital and one-year cardiac mortality after acute myocardial infarction. *Eur Heart J.* 1989;10:24-31.

67. Gjesdal O, Helle-Valle T, Hopp E, Lunde K, Vartdal T, Aakhus S, Smith HJ, Ihlen H, Edvardsen T. Noninvasive separation of large, medium, and small myocardial infarcts in survivors of reperfused ST-elevation myocardial infarction: a comprehensive tissue Doppler and speckle-tracking echocardiography study. *Circ Cardiovasc Imaging.* 2008;1:189-96, 2.

68. Kvitting JP, Wigstrom L, Strotmann JM, Sutherland GR. How accurate is visual assessment of synchronicity in myocardial motion? An In vitro study with computer-simulated regional delay in myocardial motion: clinical implications for rest and stress echocardiography studies. *J Am Soc Echocardiogr.* 1999;12:698-705.

69. Eaton LW, Bulkley BH. Expansion of acute myocardial infarction: its relationship to infarct morphology in a canine model. *Circ Res.* 1981;49:80-88.

70. Page DL, Caulfield JB, Kastor JA, DeSanctis RW, Sanders CA. Myocardial changes associated with cardiogenic shock. *N Engl J Med.* 1971;285:133-137.

71. Edvardsen T, Urheim S, Skulstad H, Steine K, Ihlen H, Smiseth OA. Quantification of left ventricular systolic function by tissue Doppler echocardiography: added value of measuring pre- and postejection velocities in ischemic myocardium. *Circulation.* 2002;105:2071-2077.

72. Skulstad H, Edvardsen T, Urheim S, Rabben SI, Stugaard M, Lyseggen E, Ihlen H, Smiseth OA. Postsystolic shortening in ischemic myocardium: active contraction or passive recoil? *Circulation.* 2002;106:718-724.

73. Urheim S, Edvardsen T, Steine K, Skulstad H, Lyseggen E, Rodevand O, Smiseth OA. Postsystolic shortening of ischemic myocardium: a mechanism of abnormal intraventricular filling. *Am J Physiol Heart Circ Physiol.* 2003;284:H2343-H2350.

74. Bugge-Asperheim B, Leraand S, Kiil F. Local dimensional changes of the myocardium measured by ultrasonic technique. *Scand J Clin Lab Invest.* 1969;24:361-371.

75. Korinek J, Vitek J, Sengupta PP, Romero-Corral A, Krishnamoorthy VK, McMahon EM, Khandheria BK, Belohlavek M. Does implantation of sonomicrometry crystals alter regional cardiac muscle function? *J Am Soc Echocardiogr.* 2007;20:1407-1412.

76. Bohs LN, Trahey GE. A novel method for angle independent ultrasonic imaging of blood flow and tissue motion. *IEEE Trans Biomed Eng.* 1991;38:280-286.

77. Garot J, Bluemke DA, Osman NF, Rochitte CE, McVeigh ER, Zerhouni EA, Prince JL, Lima JA. Fast determination of regional myocardial strain fields from tagged cardiac images using harmonic phase MRI. *Circulation.* 2000;101:981-988.

78. Hunter PJ, McCulloch AD, Ter Keurs HE. Modelling the mechanical properties of cardiac muscle. *Prog Biophys Mol Biol.* 1998;69:289-331.

79. Nash MP, Hunter PJ. Computational mechanics of the heart: from tissue structure to ventricular function. *J Elasticity.* 2000;61:113-141.

80. Streeter DD, Jr., Spotnitz HM, Patel DP, Ross J, Jr., Sonnenblick EH. Fiber orientation in the canine left ventricle during diastole and systole. *Circ Res.* 1969;24:339-347.

81. Einstein AJ, Knuuti J. Cardiac imaging: does radiation matter? *Eur Heart J.* 2012;33:573-578.

82. Bland JM, Altman DG. Statistical methods for assessing agreement between two methods of clinical measurement. *Lancet.* 1986;1:307-310.

83. Fitzmaurice GM, Ravichandran C. A primer in longitudinal data analysis. *Circulation.* 2008;118:2005-2010.

84. Curtis JP, Sokol SI, Wang Y, Rathore SS, Ko DT, Jadbabaie F, Portnay EL, Marshalko SJ, Radford MJ, Krumholz HM. The association of left ventricular ejection fraction, mortality, and cause of death in stable outpatients with heart failure. *J Am Coll Cardiol.* 2003;42:736-742.

85. Marwick TH, Leano RL, Brown J, Sun JP, Hoffmann R, Lysyansky P, Becker M, Thomas JD. Myocardial strain measurement with 2-dimensional speckle-tracking echocardiography: definition of normal range. *JACC Cardiovasc Imaging.* 2009;2:80-84.

86. Amundsen BH, Helle-Valle T, Edvardsen T, Torp H, Crosby J, Lyseggen E, Stoylen A, Ihlen H, Lima JA, Smiseth OA, Slordahl SA. Noninvasive myocardial strain measurement by speckle tracking echocardiography: validation against sonomicrometry and tagged magnetic resonance imaging. *J Am Coll Cardiol.* 2006;47:789-793.

87. Moore CC, Lugo-Olivieri CH, McVeigh ER, Zerhouni EA. Three-dimensional systolic strain patterns in the normal human left ventricle: characterization with tagged MR imaging. *Radiology.* 2000;214:453-466.

88. Nagel E, Stuber M, Burkhard B, Fischer SE, Scheidegger MB, Boesiger P, Hess OM. Cardiac rotation and relaxation in patients with aortic valve stenosis. *Eur Heart J.* 2000;21:582-589.

89. Setser RM, Kasper JM, Lieber ML, Starling RC, McCarthy PM, White RD. Persistent abnormal left ventricular systolic torsion in dilated cardiomyopathy after partial left ventriculectomy. *J Thorac Cardiovasc Surg.* 2003;126:48-55.

90. Fogel MA, Weinberg PM, Hubbard A, Haselgrove J. Diastolic biomechanics in normal infants utilizing MRI tissue tagging. *Circulation.* 2000;102:218-224.

91. Lorenz CH, Pastorek JS, Bundy JM. Delineation of normal human left ventricular twist throughout systole by tagged cine magnetic resonance imaging. *J Cardiovasc Magn Reson.* 2000;2:97-108.

92. Azhari H, Buchalter M, Sideman S, Shapiro E, Beyar R. A conical model to describe the nonuniformity of the left ventricular twisting motion. *Ann Biomed Eng.* 1992;20:149-165.

93. Durrer D, van Dam RT, Freud GE, Janse MJ, Meijler FL, Arzbaecher RC. Total excitation of the isolated human heart. *Circulation.* 1970;41:899-912.

94. Opdahl A, Helle-Valle T, Remme EW, Vartdal T, Pettersen E, Lunde K, Edvardsen T, Smiseth OA. Apical Rotation by Speckle Tracking Echocardiography: A Simplified Bedside Index of Left Ventricular Twist. *J Am Soc Echocardiogr.* 2008.

95. Becker M, Hoffmann R, Kuhl HP, Grawe H, Katoh M, Kramann R, Bucker A, Hanrath P, Heussen N. Analysis of myocardial deformation based on

ultrasonic pixel tracking to determine transmurality in chronic myocardial infarction. *Eur Heart J.* 2006;27:2560-2566.

96. Chan J, Hanekom L, Wong C, Leano R, Cho GY, Marwick TH. Differentiation of subendocardial and transmural infarction using two-dimensional strain rate imaging to assess short-axis and long-axis myocardial function. *J Am Coll Cardiol.* 2006;48:2026-2033.

97. Croisille P, Moore CC, Judd RM, Lima JA, Arai M, McVeigh ER, Becker LC, Zerhouni EA. Differentiation of viable and nonviable myocardium by the use of three-dimensional tagged MRI in 2-day-old reperfused canine infarcts. *Circulation.* 1999;99:284-291.

98. Edvardsen T, Gerber BL, Garot J, Bluemke DA, Lima JA, Smiseth OA. Quantitative assessment of intrinsic regional myocardial deformation by Doppler strain rate echocardiography in humans: validation against three-dimensional tagged magnetic resonance imaging. *Circulation.* 2002;106:50-56.

99. Hansen DE, Daughters GT, Alderman EL, Stinson EB, Baldwin JC, Miller DC. Effect of acute human cardiac allograft rejection on left ventricular systolic torsion and diastolic recoil measured by intramyocardial markers. *Circulation.* 1987;76:998-1008.

100. Stuber M, Scheidegger MB, Fischer SE, Nagel E, Steinemann F, Hess OM, Boesiger P. Alterations in the local myocardial motion pattern in patients suffering from pressure overload due to aortic stenosis. *Circulation.* 1999;100:361-368.

101. Rothfeld JM, LeWinter MM, Tischler MD. Left ventricular systolic torsion and early diastolic filling by echocardiography in normal humans. *Am J Cardiol.* 1998;81:1465-1469.

102. Stuber M, Nagel E, Fischer SE, Spiegel MA, Scheidegger MB, Boesiger P. Quantification of the local heartwall motion by magnetic resonance myocardial tagging. *Comput Med Imaging Graph.* 1998;22:217-228.

103. Henson RE, Song SK, Pastorek JS, Ackerman JJ, Lorenz CH. Left ventricular torsion is equal in mice and humans. *Am J Physiol Heart Circ Physiol.* 2000;278:H1117-H1123.

104. Cerqueira MD, Weissman NJ, Dilsizian V, Jacobs AK, Kaul S, Laskey WK, Pennell DJ, Rumberger JA, Ryan T, Verani MS. Standardized myocardial segmentation and nomenclature for tomographic imaging of the heart: a statement for healthcare professionals from the Cardiac Imaging Committee of the Council on Clinical Cardiology of the American Heart Association. *Circulation.* 2002;105:539-542.

105. Becker M, Lenzen A, Ocklenburg C, Stempel K, Kuhl H, Neizel M, Katoh M, Kramann R, Wildberger J, Kelm M, Hoffmann R. Myocardial deformation

imaging based on ultrasonic pixel tracking to identify reversible myocardial dysfunction. *J Am Coll Cardiol.* 2008;51:1473-1481.

106. Derumeaux G, Loufoua J, Pontier G, Cribier A, Ovize M. Tissue Doppler imaging differentiates transmural from nontransmural acute myocardial infarction after reperfusion therapy. *Circulation.* 2001;103:589-596.

107. Gotte MJ, van Rossum AC, Twisk JWR, Kuijer JPA, Marcus JT, Visser CA. Quantification of regional contractile function after infarction: strain analysis superior to wall thickening analysis in discriminating infarct from remote myocardium. *J Am Coll Cardiol.* 2001;37:808-817.

108. Jones CJ, Raposo L, Gibson DG. Functional importance of the long axis dynamics of the human left ventricle. *Br Heart J.* 1990;63:215-220.

109. Langeland S, D'hooge J, Wouters PF, Leather HA, Claus P, Bijnens B, Sutherland GR. Experimental validation of a new ultrasound method for the simultaneous assessment of radial and longitudinal myocardial deformation independent of insonation angle. *Circulation.* 2005;112:2157-2162.

110. Reant P, Labrousse L, Lafitte S, Bordachar P, Pillois X, Tariosse L, Bonoron-Adele S, Padois P, Deville C, Roudaut R, Dos SP. Experimental validation of circumferential, longitudinal, and radial 2-dimensional strain during dobutamine stress echocardiography in ischemic conditions. *J Am Coll Cardiol.* 2008;51:149-157.

111. Villarreal FJ, Lew WY, Waldman LK, Covell JW. Transmural myocardial deformation in the ischemic canine left ventricle. *Circ Res.* 1991;68:368-381.

112. Abraham TP, Pinheiro AC. Speckle-derived strain a better tool for quantification of stress echocardiography? *J Am Coll Cardiol.* 2008;51:158-160.

113. Bogaert J, Rademakers FE. Regional nonuniformity of normal adult human left ventricle. *Am J Physiol Heart Circ Physiol.* 2001;280:H610-H620.

114. Delfino JG, Fornwalt BK, Eisner RL, Leon AR, Oshinski JN. Determination of transmural, endocardial, and epicardial radial strain and strain rate from phase contrast MR velocity data. *J Magn Reson Imaging.* 2008;27:522-528.

115. Gallagher KP, Osakada G, Matsuzaki M, Miller M, Kemper WS, Ross J, Jr. Nonuniformity of inner and outer systolic wall thickening in conscious dogs. *Am J Physiol.* 1985;249:H241-H248.

116. Rademakers FE, Rogers WJ, Guier WH, Hutchins GM, Siu CO, Weisfeldt ML, Weiss JL, Shapiro EP. Relation of regional cross-fiber shortening to wall thickening in the intact heart. Three-dimensional strain analysis by NMR tagging. *Circulation.* 1994;89:1174-1182.

117. Helm RH, Leclercq C, Faris OP, Ozturk C, McVeigh E, Lardo AC, Kass DA. Cardiac dyssynchrony analysis using circumferential versus longitudinal

strain: implications for assessing cardiac resynchronization. *Circulation.* 2005;111:2760-2767.

118. Suffoletto MS, Dohi K, Cannesson M, Saba S, Gorcsan J, III. Novel speckle-tracking radial strain from routine black-and-white echocardiographic images to quantify dyssynchrony and predict response to cardiac resynchronization therapy. *Circulation.* 2006;113:960-968.

I

II

III